Theor Appl Climatol
DOI 10.1007/s00704-017-2223-5

ORIGINAL PAPER

High-resolution long-term WRF climate simulations over Volta Basin. Part 1: validation analysis for temperature and precipitation

Thompson Annor[1,2] · **Benjamin Lamptey**[3] · **Sven Wagner**[4,5] · **Philip Oguntunde**[2] · **Joël Arnault**[4] · **Dominikus Heinzeller**[4] · **Harald Kunstmann**[4,5]

Received: 22 December 2016 / Accepted: 6 July 2017

Abstract A 26-year simulation (1980–2005) was performed with the Weather Research and Forecast (WRF) model over the Volta Basin in West Africa. This was to investigate the ability of a climate version of WRF to reproduce present day temperature and precipitation over the Volta Basin. The ERA-Interim reanalysis and one realization of the ECHAM6 global circulation model (GCM) data were dynamically downscaled using two nested domains within the WRF model. The outer domain had a horizontal resolution of 50 km and covered the whole of West Africa while the inner domain had a horizontal resolution of 10 km. It was observed that biases in the respective forcing data were carried over to the RCM, but also the RCM itself contributed to the mean bias of the model. Also, the biases in the 50-km domain were transferred unchanged, especially in the case of temperature, to the 10-km domain, but, for precipitation, the higher-resolution simulations increased the mean bias in some cases. While in general, WRF underestimated temperature in both the outer (mean biases of −1.6 and −2.3 K for ERA-Interim and ECHAM6, respectively) and the inner (mean biases of −0.9 K for the reanalysis and −1.8 K for the GCM) domains, WRF slightly underestimated precipitation in the coarser domain but overestimated precipitation in the finer domain over the Volta Basin. The performance of the GCM, in general, is good, particularly for temperature with mean bias of −0.7 K over the outer domain. However, for precipitation, the added value of the RCM cannot be overlooked, especially over the whole West African region on the annual time scale (mean biases of −3% for WRF and −8% for ECHAM6). Over the whole Volta Basin and the Soudano-Sahel for the month of April and spring (MAM) rainfall, respectively, mean bias close to 0% was simulated. Biases in the interannual variability in both temperature and precipitation over the basin were smaller in the WRF than the ECHAM6. High spatial pattern correlations between 0.7 and 0.8 were achieved for the autumn precipitation and low spatial correlation in the range of 0.0 and 0.2 for the winter season precipitation over the whole basin and all the three belts over the basin.

Keywords High resolution · Validation · Regional climate modeling · Volta Basin · WRF · Temperature · Precipitation

1 Introduction

Assessing the impact of climate change on hydrology and water resources of the Volta Basin in West Africa has become a topical issue in recent times. On the one hand, this is as a result of various concerns raised about expected changes in the Earth's climate from global to regional scale (e.g., IPCC 2001, 2007, 2013; Jung and Kunstmann 2007; Neumann et al. 2007). On the other hand, it is due to the vital role the water resources of the Volta Basin play for the economies of the West African countries that are endowed with this natural resource. Methods such as statistical and dynamical modeling have been employed to elucidate how hydrology and water resources of the basin were impacted by the

✉ Thompson Annor
tommykak@yahoo.com

[1] Department of Physics, Kwame Nkrumah University of Science and Technology (KNUST), Kumasi, Ghana

[2] Federal University of Technology, Akure, Nigeria

[3] African Centre of Meteorological Applications for Development (ACMAD), Niamey, Niger

[4] Karlsruhe Institute of Technology, Institute of Meteorology and Climate Research, Atmospheric Environmental Research, Garmisch-Partenkirchen, Germany

[5] University of Augsburg, Augsburg, Germany

Published online: 19 July 2017

present day climate (e.g., Neumann et al. 2007; Bekoe 2013; Vigaud et al. 2011). Furthermore, these methods have been used to quantify the impact of future climate change on hydrology and water resources of the Volta Basin (e.g., Jung and Kunstmann 2007; Jung et al. 2012) utilizing various accepted future climate scenarios used in the Intergovernmental Panel on Climate Change (IPCC) third and fourth Assessment Reports IPCC (2001, 2007).

The performance of an atmospheric model depends on many factors. Giorgi (2006) for example showed that high-resolution modeling was able to simulate local circulation better than a low resolution. Jung and Kunstmann (2007), Vigaud et al. (2011), and Berg et al. (2013) ascribed improvement in simulated rainfall amounts to increase in model resolution. Frei et al. (2003) and Boberg et al. (2009, 2010) reported an enhancement in the ability of RCMs to capture precipitation intensities due to increase in the model resolution. It can therefore be said that high spatial resolution RCM simulations could provide better representations of small-scale features such as local circulation and topography (Giorgi 2006), rainfall amount (Jung and Kunstmann 2007; Vigaud et al. 2011; Berg et al. 2013), and precipitation intensity (Frei et al. 2003; Boberg et al. 2009, 2010). Nevertheless, the improvement in simulating all the fields in the model cannot be credited to increase in resolution alone as asserted by Giorgi (2006) and Berg et al. (2013). Additionally, studies on added value (AV) of RCMs (e.g., Castro et al. 2005; Feser 2006; Winterfeldt and Weisse 2009; Prömmel et al. 2010; Veljovic et al. 2010; Mariotti et al. 2011; Di Luca et al. 2012, 2013; Giorgi and Gutowski 2015) indicate that while some aspects of a GCM can be enhanced, other aspects of the same GCM can also be marred by the high-resolution RCM simulations. Specifically, locations where the climate indicator is influenced to large extent by the neighboring forcing tend to have AV in the RCM simulation (Nikulin et al. 2012; Giorgi and Gutowski 2015; Prein et al. 2016). On the other hand, AV, in general, is not observed in the RCMs for areas having their climate controlled by large-scale external features (Torma et al. 2015; Giorgi and Gutowski 2015).

Hydrological models are usually employed to assess the impact of climate change on river basin hydrology. Such impact models are required to be driven by high spatial (Senatore et al. 2010; Jung et al. 2012) and temporal resolution climate simulations. The spatial resolutions of available global climate models (e.g., Roeckner et al. 2006) are low and usually not suitable for use as climate input data for impact studies models. In low spatial resolution simulations, features and interaction processes such as digital elevation model (DEM), unique localized circulations due to topography which are crucial for climate impact studies are not appropriately resolved (Nikulin et al. 2012; Giorgi and Gutowski 2015; Prein et al. 2016). It has also been shown that the high temporal resolution that are found in RCM simulations improve the representation of precipitation extremes especially on the diurnal and seasonal time scales (Giorgi and Gutowski 2015; Prein et al. 2016). Vital among these features and interaction processes to hydrological modeling is the DEM which is used to derive the needed river catchment networks. Also, one remarkable feature over the West African region is the high spatial variability in precipitation at the scale where impact studies are required. Furthermore, high-resolution simulation of precipitation may be beneficial for hydrological modeling of the basin. Consequently, the need for high-resolution regional climate model simulation is paramount for an area such as the Volta Basin where a lot of benefits are derived from its water resources.

In an attempt to address this issue, some studies regarding regional climate model (RCM) simulations over the basin and the West African region had been conducted. Kunstmann and Jung (2005) for instance applied the Fifth-Generation of the Mesoscale Model MM5 (Grell et al. 1995) with the Oregon State University-Land Surface Model (OSU-LSM) (Chen and Dudhia 2001) to simulate temperature, precipitation, evapotranspiration, and surface runoff for 1990–1999 and 2030–2039. They reported strong regional differences in the projected changes of these variables over the whole basin. Also, Jung and Kunstmann (2007), Kasei (2009), and Jung et al. (2012) applied impact study models forced/coupled with RCM outputs to study the hydrological impact of climate change over the Volta Basin for a present-day 10-year period and another 10-year period in the future. Sylla et al. (2009) reported an enhanced representation of precipitation and temperature over West Africa for the 1981–2000 period when the Regional Climate Model version 3 (RegCM3) was used to downscale two large-scale GCMs. Furthermore, Vigaud et al. (2011) applied WRF to project the changes in the West African climate between the 1981–1990 and 2032–2041 periods and showed that critical climate features of the West African region were simulated better in the RCM than the forcing large-scale model. Nikulin et al. (2012) used 10 RCMs all forced by a reanalysis data and reported an added value in some RCMs over the large-scale reanalysis driving data over certain parts of West Africa especially on the diurnal and seasonal scale. There is no doubt of the usefulness of these studies for the West African region in general and the Volta Basin in particular, but the period for the simulations in most cases was short (mostly 10 years) for adequate climate analysis and also in some cases the horizontal resolution in the RCM simulations were low. It is therefore very important to have long-term RCM simulations with high spatial resolution which can be used for rigorous climate change analysis and can also provide the long-term atmospheric forcing data for impact studies over the basin.

In this study, long-term high-resolution regional climate simulations for the Volta Basin were performed. Here, WRF was used to dynamically downscale a reanalysis dataset (the ERA-Interim) and one of the GCMs used in the IPCC's Fifth Assessment Report IPCC-AR5 (IPCC 2013) the Max Planck

Institute Earth System Model (MPI-ESM/ECHAM6). In order to have confidence in the RCM to simulate possible future change and variability in the climate of the Volta Basin, present-day climate simulations were conducted to assess the performance of the RCM in reproducing the climate of the Volta Basin with respect to temperature and precipitation. There are usually two main steps required for climate projection: (1) validation of the model for past and present climate and (2) future climate simulation with the previously validated climate model and this paper focuses on the first step.

In this paper, the validation of the WRF RCM dynamical downscaling of the ERA-Interim and the ECHAM6 with observational data are presented. Section 2 discusses the observational data and the models used for the study. Section 3 first focuses on the evaluation of the ERA-Interim driven simulations at 50 and 10 km followed by the evaluation of the ECHAM6 GCM output and the WRF driven by the ECHAM6 for the 50- and 10-km simulations. The summary and conclusions are found in section 4.

2 Data and models

2.1 Observational data

The spatial density of observed precipitation data is crucial for the West Africa region due to the highly varying spatial distribution of precipitation over the region. Ironically, the availability of high-quality dataset especially in the case of precipitation over the region is problematic, as several studies (e.g., Nicholson 2003; Paeth et al. 2011; Nikulin et al. 2012) have alluded to this fact. This problem is further compounded by the fact that gauge station precipitation data over West Africa are measured by meteorological agencies of the respective countries within the region, and the individual meteorological agencies of these states have their own policies about data acquisition and usage. The policies of these agencies make it difficult to obtain station gauge observational precipitation and temperature data for the study areas from them. Hence, gridded observational open source data sets become the practical option in most cases for model validation purposes within the region. Widely used open source precipitation data include those from the Climate Research Unit (CRU), the Global Precipitation Climatology Centre (GPCC), the Global Precipitation Climatology Project (GPCP), Tropical Rainfall Measuring Mission (TRMM), and Climate Prediction Center morphing technique (CMORPH). These data sets are made up of purely gridded gauge station data in some cases, and in other cases, satellite estimates are merged with gauge data. Due to the different methods applied in the gridding process, the number of stations available and various algorithms employed in case of the satellite estimates, uncertainties exist in these observational data. The spread in the uncertainties is wider on the local scale than the large-scale precipitation features (Gruber et al. 2000; Fekete et al. 2004; Nikulin et al. 2012). Nikulin et al. (2012) reported a good agreement between GPCC and GPCP (bias from 0 to −0.5 mm/day) over the study area for the January, February, and March season of the 1998–2008 climatology showing the robustness of the GPCC data. In addition, there are quite a significant number of gauge stations from West Africa that are incorporated in the development of the GPCC data set. Studies such as Nicholson (2003), Paeth et al. (2011), and Dinku et al. (2008) have also demonstrated the robustness of GPCC. Therefore, the GPCC version 6.0 (Schneider et al. 2011) was used to validate the precipitation output from the models. The data consists of monthly total precipitation at 0.5° horizontal resolution covering the land surface of the entire globe. The precipitation data, however, has low station density over the Sahara region, Liberia and Sierra Leone (Nikulin et al. 2012). For temperature, the version TS3.21 (Harris et al. 2013) dataset of the Climate Research Unit (CRU) was used to compare near surface air temperature for the GCM and the RCM simulations. At 0.5° spatial resolution over the land surface of the earth, the temperature data set uses station measurements from weather agencies across the globe to develop the monthly mean temporal resolution of the temperature dataset (Harris et al. 2013). Previous studies had also used these datasets for model validation over the region (e.g., Jung and Kunstmann 2007; Sylla et al. 2009). However, the uncertainty in the observational dataset should be considered over those areas where high-quality observational data is not available, since this can affect the evaluation of the model performance.

2.2 Model data

The MPI-ESM (ECHAM6/MPIOM) GCM (Giorgetta et al. 2013) was selected for this study based on its consistent appearance in the Coupled Model Inter-comparison Project (CIMP). Additionally, the good overall performance of the previous versions of the GCM over West Africa and the Volta Basin has been confirmed by some studies (e.g., Jung and Kunstmann 2007; Sylla et al. 2009; Oguntunde and Abiodun 2013; Annor 2015). A non-hydrostatic RCM model, the Weather Research and Forecasting (WRF) model (Skamarock et al. 2008), was used for the downscaling of the GCM. Two nested domains of 50- and 10-km horizontal resolution were used in the RCM. The outer domain covered the whole of West Africa, while the higher-resolution inner domain is centered over the Volta Basin (Fig. 1). A brief description of the GCM and RCM used in the study is given in the following two subsections. To assess the biases due to the RCM itself and to remove the biases resulting from the GCM driving data, control simulations were performed, in which the WRF model was used to downscale the ERA-Interim reanalysis data (Dee et al. 2011) with exactly the same configuration as in the case of the GCM downscaling simulation.

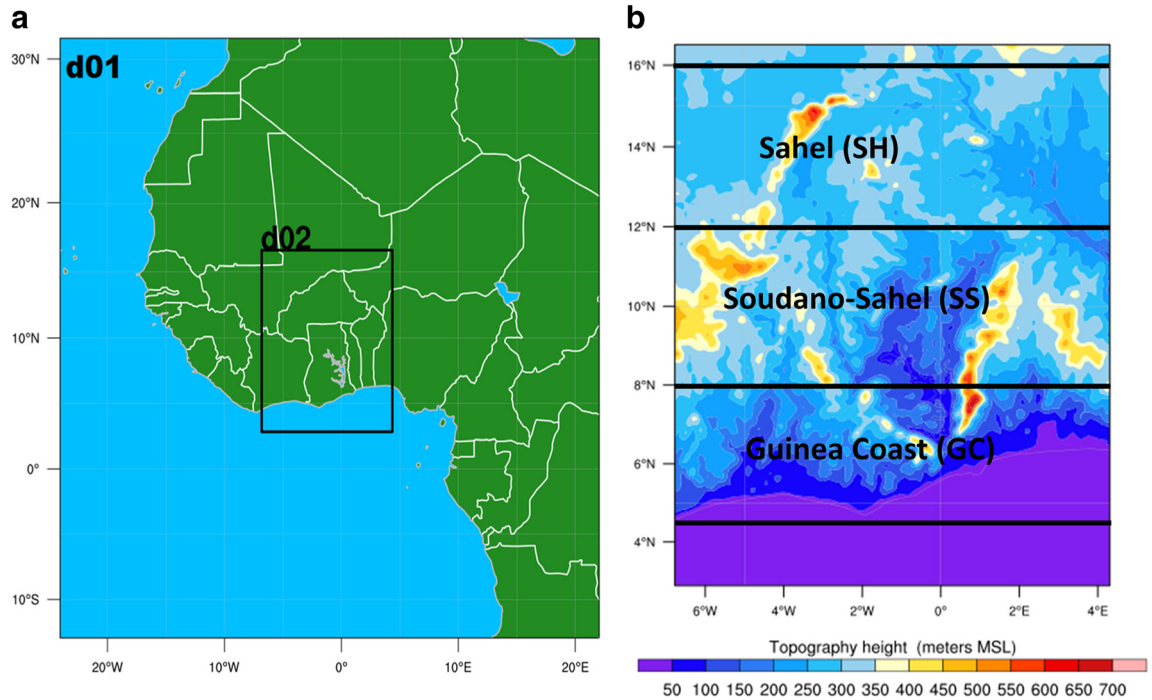

Fig. 1 Geographical map indicating the two domains used in the WRF simulation experiments (**a**). The outer/coarser resolution domain is marked with d01, and the inner/higher resolution domain is marked with d02. The three sub-regions are shown in **b**. NCAR Command Language (NCL) package was used for this figure

2.2.1 The MPI-ESM (ECHAM6/MPIOM) model

The MPI-ESM (ECHAM6/MPIOM) GCM, the new version of the ECHAM series of atmospheric and oceanic general circulation models developed based on ECHAM5 (Roeckner et al. 2003; Roeckner et al. 2006), was selected for this work. It has an embedded land vegetation model the JSBACH (Raddatz et al. 2007) which includes parameterizations of physical processes and a hydrological discharge model that take care of river runoff to the oceans (Giorgetta et al. 2013). The realization one of the historic simulations of the Max Planck Institute Earth System Model running on Medium Resolution (MPI-ESM-MR) (Giorgetta et al. 2013) was downscaled. The model forms part of version 5 of the Coupled Model Inter-comparison Project (CMIP5) managed by the World Climate Research Programme (http://cmip-pcmdi.llnl.gov/cmip5) that was used for the IPCC-AR5. The model was run at T63 (i.e., 1.9° or ~200 km) horizontal resolution with 95 vertical levels up to 1 Pa. Anthropogenic greenhouse gases, starting from pre-industrial conditions, were used to force the GCM (Giorgetta et al. 2012, 2013; Annor 2015).

2.2.2 The weather research and forecasting model

The version 3.5.1 of the terrain following WRF model (Skamarock et al. 2008) was employed for the nested high-resolution climate simulation over the Volta Basin. Atmospheric fields such as pressure, wind, temperature, and sea surface temperature (SST) from the GCM were used to drive the WRF (Annor 2015). The RCM simulations applied the time-varying SST, sea ice, soil moisture, vegetation fraction, and albedo (Skamarock et al. 2008) option with inputs from the respective large-scale forcing data.

A double-nested approach on a Mercator map projection was used. The outer domain had 100 × 100 grid points at 50-km horizontal resolution, covering the whole of West Africa. At 10-km horizontal resolution centered over the Volta Basin, the inner domain had 151 grid points in north-south and 121 grid points in east-west direction (Fig. 1). The vertical stratification used 35 vertical levels for both domains with the top of both nests at a pressure of 20 hPa (Annor 2015). We used a specified condition where relaxation zone has 4 points.

Based on a series of 3-year period test simulations for both domains and sensitivity investigation simulations previously performed for West Africa using WRF (e.g., Noble et al. 2014), the options of physics schemes in Table 1 were selected and applied in the simulation experiment of the 1979–2005 period. A time step of 240 s was used for the outer domain integration with a 10-min radiation time step. The first 1 year of the simulation was discarded as spin up, and for that matter, the 1980–2005 period was used for the analysis in this study.

3 Results

In order to validate the performance of the RCM, the ERA-Interim reanalysis data was first used as boundary forcing data

Table 1 Selected options of physics schemes used for the simulation experiment

Physics scheme	Selected scheme option
Microphysics	WRF Single–Moment 5–class (Hong et al. 2004)
Longwave	Rapid Radiative Transfer Model (RRTM) longwave (Mlawer 1997)
Cumulus	Grell–Devenyi (GD) ensemble (Grell and Devenyi 2002),
Shortwave	Dudhia shortwave (Dudhia 1989)
Planetary boundary layer physics	Asymmetric Convection Model 2 (ACM2) (Pleim 2007)
Land surface model	Unified Noah land surface model (Tewari et al. 2004)
Surface layer	MM5 Similarity (Dyer and Hicks 1970; Paulson 1970; Webb 1970; Zhang and Anthes 1982; Beljaars 1994)

for both the outer domain (hereafter called WRF_ERA_50) and the inner domain (hereafter called WRF_ERA_10). This was done to assess the performance of the RCM under perfect-prognosis conditions. In a second step, the MPI-ESM (or ECHAM6) data was used as lateral boundary conditions for the outer domain (hereafter called WRF_ECHAM6_50) and the inner domain (hereafter called WRF_ECHAM6_10). Furthermore, precipitation and temperature data of the GCM (henceforth named ECHAM6_50 for the outer and ECHAM6_10 for the inner domains, although, both domains have the same resolution) are presented to allow for the identification of the origin of differences in the results between the WRF_ERA and the WRF_ECHAM6 runs. The results for both domains used in this study are presented here, but emphasis is given to the 10-km target domain over the basin of this study. For the analysis in the outer domain, regridding of the GCM and observation data sets are done onto 50-km grids using the nearest neighbor interpolation method, whereas in the case of the inner domain analysis, the GCM and observation data were interpolated onto 10-km grids using the nearest neighbor method.

3.1 WRF simulation with ERA-interim boundary conditions

3.1.1 Temperature and precipitation results for the outer domain

The outer domain results for the 1980–2005 climatological mean bias of annual mean 2-m temperature (ERA_50 minus CRU and WRF_ERA_50 minus CRU) and annual total precipitation (ERA_50 minus GPCC and WRF_ERA_50 minus GPCC) are shown in Fig. 2.

WRF produces a cold bias for most areas of the domain with an average value of 1.59 K. The cold bias intensifies in the Sahara region (latitudes greater than 16° N). However, the performance of the model is improved in regions south of latitude 16° N, where the bias ranges from 0 to −1.5 K for most areas. The temperature gradient generated by the WRF model between the Sahara and the coastal regions has also been reported in previous regional climate simulation studies (e.g., Sijikumar et al. 2006; Vigaud et al. 2011) performed over West Africa. A possible reason for the large cold bias (−2.0 to −4.8) simulated by the RCM over the Sahara could be linked to the simulation of a higher than usual albedo for this region than elsewhere based on the huge dust aerosols found there. Hence, the reflection of solar radiation back into space is higher over the Sahara than the south of latitude 16° N, resulting in the simulation of lower temperatures. Studies performed by Mooney et al. (2013) and Katragkou et al. (2015) attributed a general cold bias in WRF to the NOAH LSM. Therefore, the general underestimation of temperature over almost the entire domain by the WRF model could be due to the NOAH LSM scheme used in this study. A look at the spatial bias in the forcing data (Fig. 2a) points to the internal model physics as the reason for the cold bias in the WRF simulation.

The simulated annual precipitation over the outer domain produced dry bias (up to −90%) in almost the entire region above latitude 16° N in the WRF_ERA_50. On the other hand, the model simulated the observed precipitation quite well over the southern part of the domain, especially over Ghana, Burkina Faso, Togo, Benin, parts of Nigeria, and of the Ivory Coast. However, a weak wet bias is produced in the south-east of the outer domain. The dry bias mostly over the northern part of the domain in the forcing data (Fig. 2c) persists in the WRF_ERA_50 simulation (Fig. 2d) though dry bias is simulated for wider area in the WRF simulation. Below latitude 16° N, the WRF simulates the observed precipitation quite better than the forcing data. Nikulin et al. (2012) reported large positive bias of precipitation over southern part of West Africa when the WRF model was driven by the ERA-Interim data. In this study, the WRF model simulates the observed precipitation quite well compared to their simulation over the same area of the region. In the northern and eastern parts of the West African region, our results are consistent with theirs. The use of the different physics schemes might have accounted for the differences in the simulation of precipitation over the southern part of the domain. Also, the biases simulated here are comparable to those reported by Giorgi et al. (2012) for the region.

3.1.2 Temperature and precipitation results for the Volta Basin of the 10-km domain

The Volta Basin in the inner domain is masked for the analysis of temperature and precipitation. Figure 3a shows the 1980–2005 period climatological mean bias in annual mean 2-m temperature over the Volta Basin.

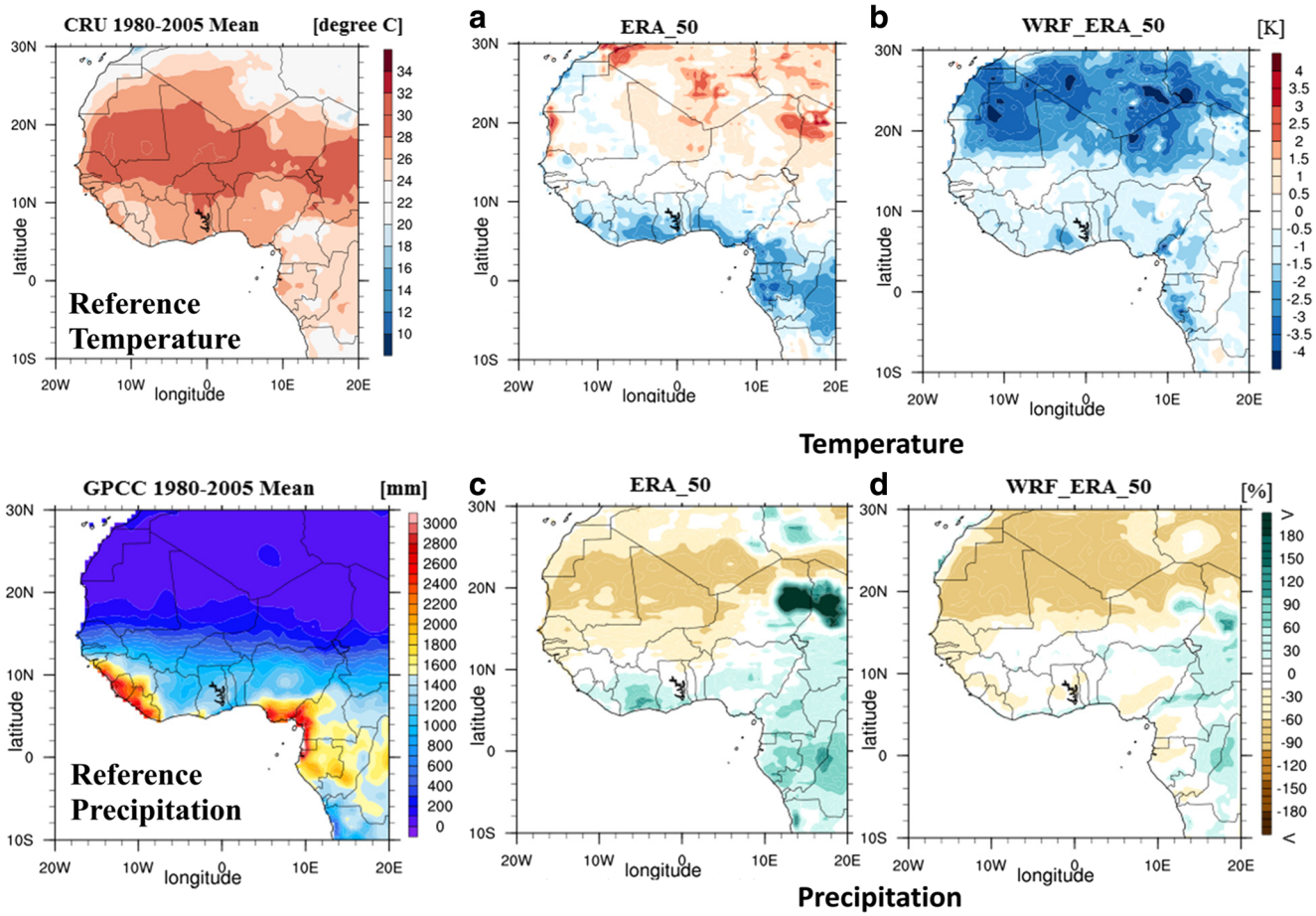

Fig. 2 Difference (i.e., model minus observation) maps of 1980–2005 climatological mean of annual mean temperature (**a**, **b**) and annual total precipitation (**c**, **d**) for ERA_50 and WRF_ERA_50 in comparison with CRU data for temperature and GPCC data for precipitation. NCAR Command Language (NCL) package was used for this figure

In general, over the entire basin, the RCM shows a weak cold bias in 2-m temperature, ranging from 0 to −1 K. However, along the south-western and south-eastern boundaries of the domain, the cold bias intensifies up to −2.5 K. The underestimation of observed temperature by the model over the whole basin for the inner domain simulation is consistent with the cold bias

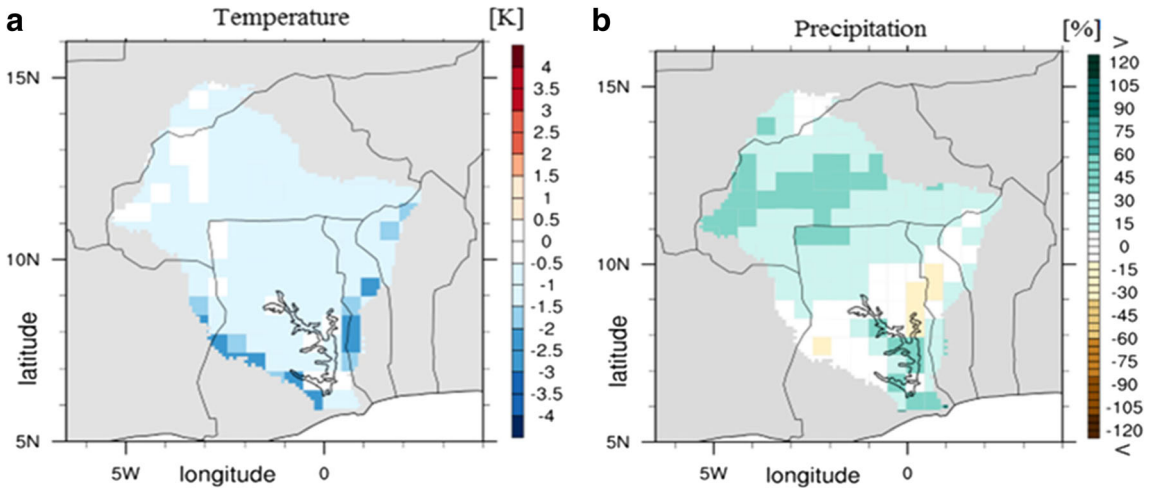

Fig. 3 Difference (i.e., model minus observation) maps of 1980–2005 climatology of annual mean temperature (**a**) and annual total precipitation (**b**) for the WRF_ERA_10 in comparison with CRU data for temperature and GPCC data for precipitation, for the Volta Basin. NCAR Command Language (NCL) package was used for this figure

simulated by the model over the same region within the 50-km domain (i.e., the nesting approach did not introduce a further bias for the 2-m temperature). The WRF_ERA_10 reasonably simulated the 2-m temperature on the annual scale over the Volta Basin, and this result is consistent with previous simulations performed over the basin. For instance, Jung and Kunstmann (2007) reported bias in the range of −2 to 2 °C over the Volta Basin for 2-m temperature using the MM5 model.

Figure 4 indicates the period climatological mean bias in seasonal mean 2-m temperature over the basin. The observed temperature is generally underestimated over most parts of the basin in all the seasons which is quite similar in pattern to that of the annual time scale. However, for the March to May (MAM) season, the bias for larger area of the basin is close to zero, while the model simulates bias up to 2 K over the northern part of the basin for the June to August (JJA) season.

Table 2 summarizes the seasonal means for the 2-m temperature over the Volta Basin of the WRF_ERA_10. The mean bias is negative for all seasons, leading to an annual mean bias of −0.9 K simulated by the RCM. The WRF model shows the smallest bias of −0.6 K for the MAM season and the largest bias of −1.1 K for the September, October, and November (SON) season. It is worth mentioning that the nested simulation over the Volta Basin does not substantially change the bias in 2-m temperature on the seasonal time scale compared to the outer domain. This is consistent with our

Table 2 Inner domain seasonal and annual mean 2-m temperature mean bias [K] in comparison with CRU temperature version TS3.21, averaged over the entire Volta Basin from 1980 to 2005 for the WRF_ERA_10 and WRF_ERA_50

	DJF	MAM	JJA	SON	Annual
WRF_ERA_10	−1.0	−0.6	−0.7	−1.1	−0.9
WRF_ERA_50	−1.1	−0.4	−0.6	−1.0	−0.8

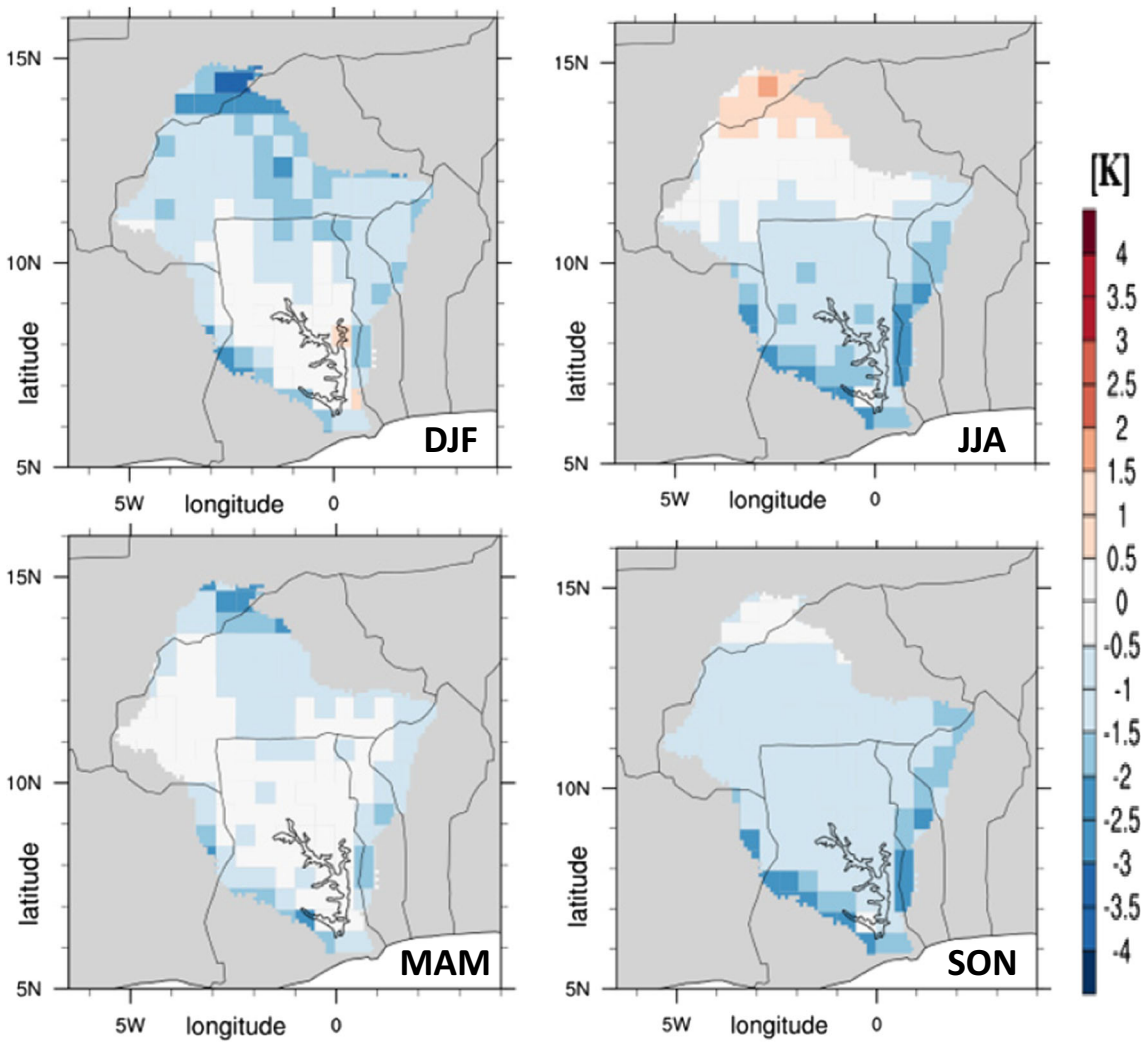

Fig. 4 Difference (i.e., model minus observation) maps of 1980–2005 climatology of seasonal mean temperature for the WRF_ERA_10 in comparison with CRU data over the Volta Basin. NCAR Command Language (NCL) package was used for this figure

earlier assertion that the WRF_ERA_10 keeps the systematic bias in 2-m temperature somehow constant. The general cold bias simulated over the basin and over the 50-km domain on the seasonal scale has also been reported in previous dynamical downscaling of reanalysis data with RCMs over West Africa (e.g., Sylla et al. 2009).

The results for the interannual variability in 2-m temperature averaged over the basin are given in the top panel of Fig. 5. For the WRF_ERA_10 simulation, with the exception of few years (1980, 1985, 2003, and 2004) where the observed interannual variability is out of phase with the one simulated, the observed interannual variability over the period is fairly reproduced both in pattern and values (with the least biases). The increasing trend in the observed temperature is also well captured in the WRF_ERA_10 simulation. Also, the WRF_ERA_10 simulation is able to reproduce well the observed hottest (coldest) temperature in 1987 (1992).

With respect to total annual precipitation (Fig. 3b), an average wet bias of approximately 20% is produced for the entire basin. Larger bias of about 40% is produced in few areas like central part of Burkina Faso and over the Volta Lake. However, over south-western and central-eastern parts of Ghana, most parts of the basin in Togo, Benin, and Mali, the WRF model simulated the observed precipitation quite well. For the same region (i.e., the Volta Basin), the underestimation of observed precipitation on the annual scale is slightly improved in the WRF_ERA_10 simulation. The reason therefore could come from the PBL scheme, which is seeing stronger orographic features due to a better resolution of the topography in the inner domain (Frei et al. 2003; Vigaud et al. 2011; Boberg et al. 2009, 2010). In addition, the convective scheme could also contribute to the increased wet bias in the 10-km domain of the basin as Afiesimama et al. (2006), attributed a wet bias within the Guinea Coast of the basin to the convective scheme. This study is compared in terms of model biases over the region, to previous RCM simulations performed by Jung and Kunstmann (2007) (it should be noted that the periods of the two studies are not the same). Biases are of similar level of magnitude and in some cases smaller in this study. For instance, a bias ranging from 0 to 45% is produced in most areas in this study, whereas a dry bias was generally produced over the same area in their study and furthermore, a bias up to around −120% was produced over the Guinea Coat of the basin in their simulations.

The spatial bias results for the seasonal total precipitation (Fig. 6) show that the observed precipitation is underestimated (bias between 15 and −105%) over almost the entire basin for the December to February (DJF) season. Conversely, the observed precipitation is overestimated (bias between −15 and 120%) over almost the entire basin in case of the MAM season. For the JJA season, model simulates a weak positive bias over the almost entire Burkina Faso and the northwestern parts of Ghana of the basin, but a weak negative bias in the eastern part of the basin. Among all the seasons, the JJA has the largest area with bias close to zero followed by the

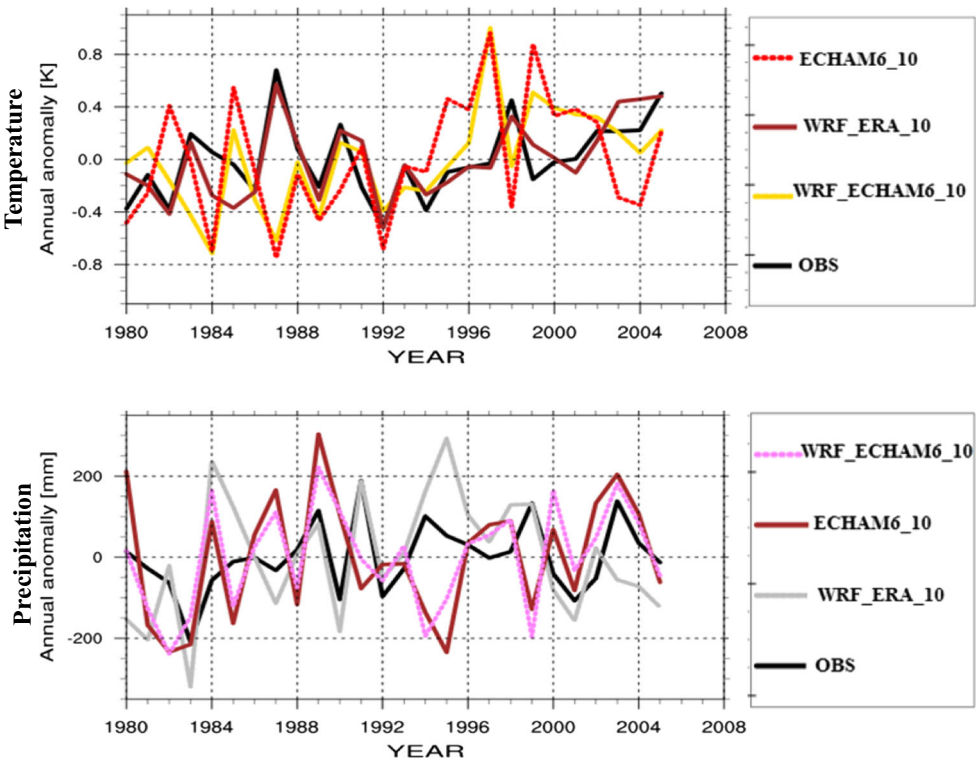

Fig. 5 Time series of the interannual variability for temperature (*top*) and precipitation (*bottom*) of the 10-km simulation averaged spatially over the Volta Basin. The anomaly is calculated using the mean for the 1980–2005 period. NCAR Command Language (NCL) package was used for this figure

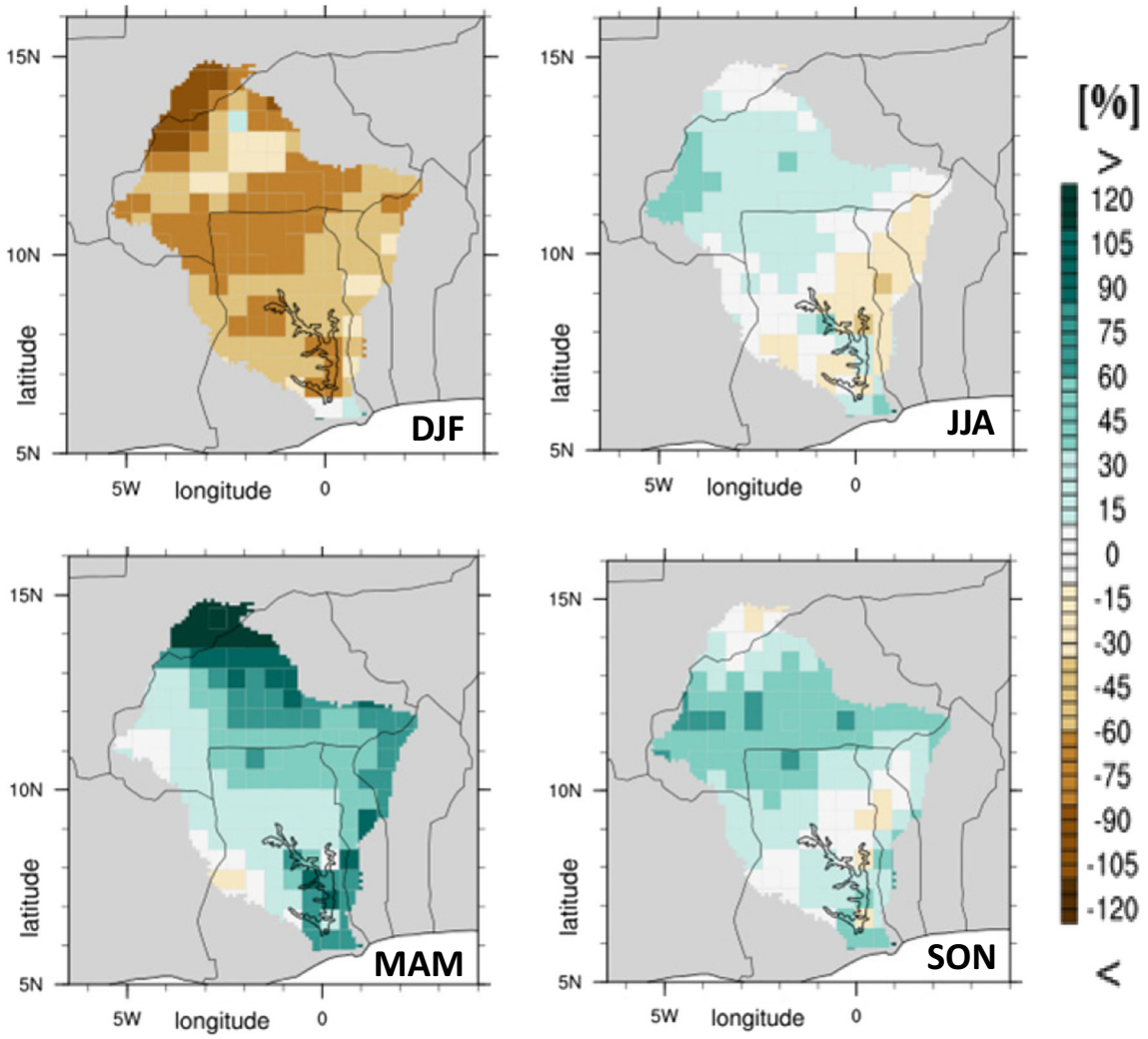

Fig. 6 Difference (i.e., model minus observation) maps of 1980–2005 climatology mean of seasonal total precipitation for the WRF_ERA_10 in comparison with GPCC data over the Volta Basin. NCAR Command Language (NCL) package was used for this figure

September to November (SON) season. Similar to the JJA season, the SON season also recorded positive bias (quite stronger than the JJA season) over almost all parts of Burkina Faso.

The month of April is a crucial month as far as the climate of the Volta Basin, and the whole of West Africa region is concerned. April marks the transition between the dry and wet seasons (see Fig. 7) and therefore is regarded mainly as the month in which the onset of the rainy season occurs (see Jung and Kunstmann 2007; Vigaud et al. 2011) in the region. In light of this, the results of the inner domain for the 1980–2005 climatological mean bias in April total precipitation are shown in Fig. 8.

Averaged over the entire basin (Fig. 8), the WRF_ERA_10 simulates a relative wet bias of about 68% for the month of April. The north-eastern, eastern, and south-eastern portions, including the central part of the Volta Basin, have positive biases, and the bias is the largest (>120%) mainly in the north-eastern part of the basin. On the other hand, a bias between 0 and −26% is produced at the western boundary of the 10-km domain. A careful look at the large wet bias simulated by the model over the north-western and south-western parts of the domain suggests that the model places the onset of the rainy season in April over the entire basin. It is, however, known that the Savannah-type regions over the Volta Basin (in this case, areas where biases are largely positive) generally have a later start of the wet season (Amisigo 2005). Therefore, the large wet bias can be attributed to model deficiencies.

The seasonal means of precipitation of the WRF_ERA_10 are shown in Table 3. The Volta Basin is divided into three regions in accordance with Sylla et al. (2009) (also see Fig. 1). Hence, the WRF_ERA (VB), WRF_ERA (GC), WRF_ERA (SS), and the WRF_ERA (SH) are the seasonal means for the whole Volta Basin, for the Guinea Coast, the Soudano-Sahel, and the Sahel regions, respectively, of the ERA-Interim driven simulation. The RCM simulated wet bias for all seasons except winter (DJF) for all regions and summer (JJA) over the

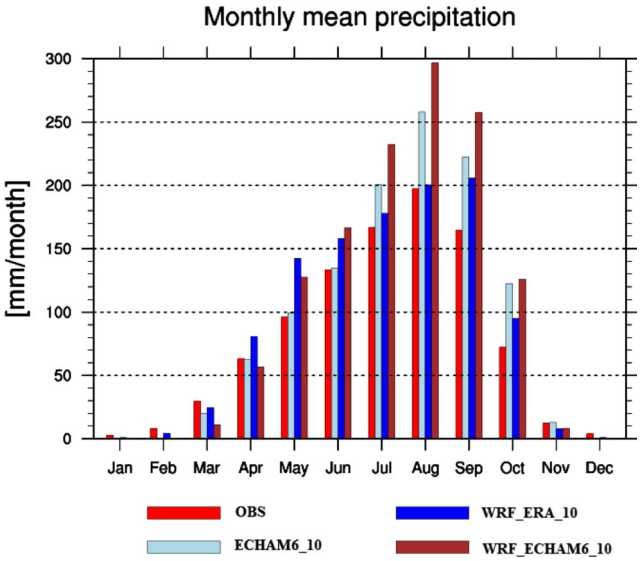

Fig. 7 The annual cycle (1980–2005 climatological mean) of monthly total precipitation averaged over the Volta Basin of the 10-km domain for observation (GPCC), WRF_ERA_10, WRF_ECHAM6_10, and ECHAM6_10. NCAR Command Language (NCL) package was used for this figure

Guinea Coast. The WRF model shows larger biases for the winter (DJF) and spring (MAM) seasons than the summer (JJA) and autumn (SON) seasons. In general, mean biases in precipitation are smallest for the summer season and largest for the month of April over the basin. With respect to the three sub-regions, the WRF_ERA_10 simulation produced smallest (largest) mean biases over the Guinea Coast (Sahel). In the test simulation prior to the selection of an optimal configuration for this study, we found that the simulation of precipitation over the Guinea Coast and the Sahel regions is highly sensitive to the cumulus scheme. Hence, the difference in mean biases presumably arises from the suitability of the chosen cumulus scheme for the respective region. The 10-km

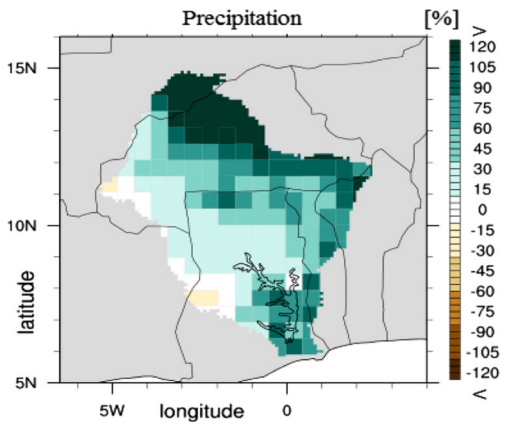

Fig. 8 Difference (i.e., model minus observation) maps of 1980–2005 climatology of April total precipitation for the WRF_ERA_10 in comparison with GPCC data, for the Volta Basin. NCAR Command Language (NCL) package was used for this figure

Table 3 April, seasonal, and annual total precipitation relative bias [%] of the inner domain, in comparison with GPCC version 6.0 data, averaged over the entire Volta Basin (VB), the Guinea Coast (GC), the Soudano-Sahel (SS), and the Sahel (SH) regions of the Volta Basin from 1980 to 2005 for WRF_ERA_10 and WRF_ERA_50

Simulation	April	DJF	MAM	JJA	SON	Annual
WRF_ERA_10 (VB)	70	−58	52	8	28	20
WRF_ERA_50 (VB)	34	61	33	−13	7	−3
WRF_ERA_10 (GC)	53	−45	46	−1	21	17
WRF_ERA_50 (GC)	18	−64	10	−17	−5	−12
WRF_ERA_10 (SS)	46	−58	39	6	29	17
WRF_ERA_50 (SS)	18	−131	12	−16	8	−6
WRF_ERA_10 (SH)	132	−63	89	20	31	27
WRF_ERA_50 (SH)	86	373	56	3	12	9

simulation reduces the mean biases averaged over the whole basin and the three belts for the DJF and JJA (except SH) seasons. For the MAM, SON seasons, April, and the annual totals, the high-resolution simulation increases the mean biases over the whole basis and the three belts. The reason for the reduction in the biases could be that the beneficial effect of the 10-km simulation in representing the subgrid surface features surpasses the mar effect of the one-way nested approach. In the situations where biases are increasing in the 10-km simulation, the reverse is the case.

The results for the interannual variability in precipitation averaged over the basin are given in the bottom panel of Fig. 5. The WRF_ERA_10 simulates fairly well the observed temporal pattern in the interannual variability. However, the biases in the amplitude of the variability are quite large in some years (1980–81, 1983–84, 1995, and 2003). On the other hand, the amplitude of the simulated interannual variability matches well the observation for the 1988–1993 and 1999–2002 periods. The driest (1983) and the wettest (1991) years within the period are fairly captured (well captured in the wettest year) in the WRF_ERA_10 simulation.

3.2 Simulation with ECHAM6 boundary conditions

Additional biases are usually introduced in dynamical downscaling processes when RCMs are driven by GCMs. Thus, the bias in the ECHAM6 GCM downscaling experiment for 2-m temperature and precipitation is also presented here as a way of tracing the propagation of the bias in the downscaling chain. It is important, however, to note that the GCM parameters used in forcing the RCM do not include 2-m temperature and precipitation. Therefore, the bias produced in these fields can have various sources and are not a good indicator for the bias in the forcing fields of atmospheric pressure, temperature, and wind provided at the lateral boundaries by the GCM. The results will, however, contribute towards understanding the performance of the WRF model over West Africa.

3.2.1 Outer domain temperature and precipitation results

In general, temperature is underestimated (see Fig. 9b, average bias of about −0.7 K) by the MPI-ESM (figure named ECHAM6_50). However, some areas, mainly in the western part of the Sahara region, have overestimated temperature by 0.5–4.6 K. Over some areas, especially in the Sahel and remaining Sahara region, MPI-ESM is producing nearly a null bias in 2-m temperature. In the case of the WRF simulations (Fig. 9c), the cold bias in 2-m temperature of the GCM is intensified (domain average of about −1.6 K). Over the Sahel and the Sahara regions (parts of the domain lying north of latitude 14° N), the observed temperature is strongly underestimated, whereas the underestimation is quite weak over the Guinea Coast and the Soudano-Sahel (i.e., regions south of latitude 14° N). Around the Volta Lake, the RCM reproduces the 2-m temperature better than the GCM. This can be attributed to an improved representation of the Volta Lake in the RCM simulation. The spatial distribution of the 2-m temperature bias of the WRF_ECHAM6_50 is similar to the WRF_ERA_50 simulations confirming the effect of the LSM scheme applied for this study. However, the reference (CRU) temperature is strongly underestimated in the case of WRF_ECHAM6_50. It is evident that the RCM simulation for the 50-km domain increased the mean bias in the 2-m temperature. It is known that an improved representation of subgrid- and small-scale features like topography, clouds, and local circulation benefit significantly from a high horizontal resolution (Frei et al. 2003; Vigaud et al. 2011; Boberg et al. 2010; Berg et al. 2013). However, it is equally important to point out that not all physical processes can be simulated well as a result of an increased horizontal resolution (Giorgi 2006). Thus, our results suggest that large-scale features that are represented quite well in the GCM influence the simulation of 2-m temperature over the outer domain more than increase in horizontal resolution does. Also, internal model physics of the WRF might have contributed in the general cold bias simulated for temperature.

The bias in annual total precipitation with respect to the 1980–2005 GPCC climatology is shown in the bottom panel of Fig. 9. The MPI-ESM results for precipitation (Fig. 9e) are mainly dry (with a relative bias between 0 and −95%) in the Sahara region. On the other hand, a wet bias from 0 up to 90% is visible for most areas of the Guinea Coast and the Soudano-Sahel, except the western ends of these regions, which show a dry bias of around 30%. The RCM simulation, however, reduces the mean relative bias of the GCM from −8% (averaged over the whole domain) to about −3% for total annual precipitation. The general dryness in most parts of the Sahara and wetness in many parts of the Guinea Coast still persist in the RCM downscaling experiments, which demonstrates the influence of the GCM forcing data on the RCM simulations. Also, the overall wet bias that persists in the Guinea

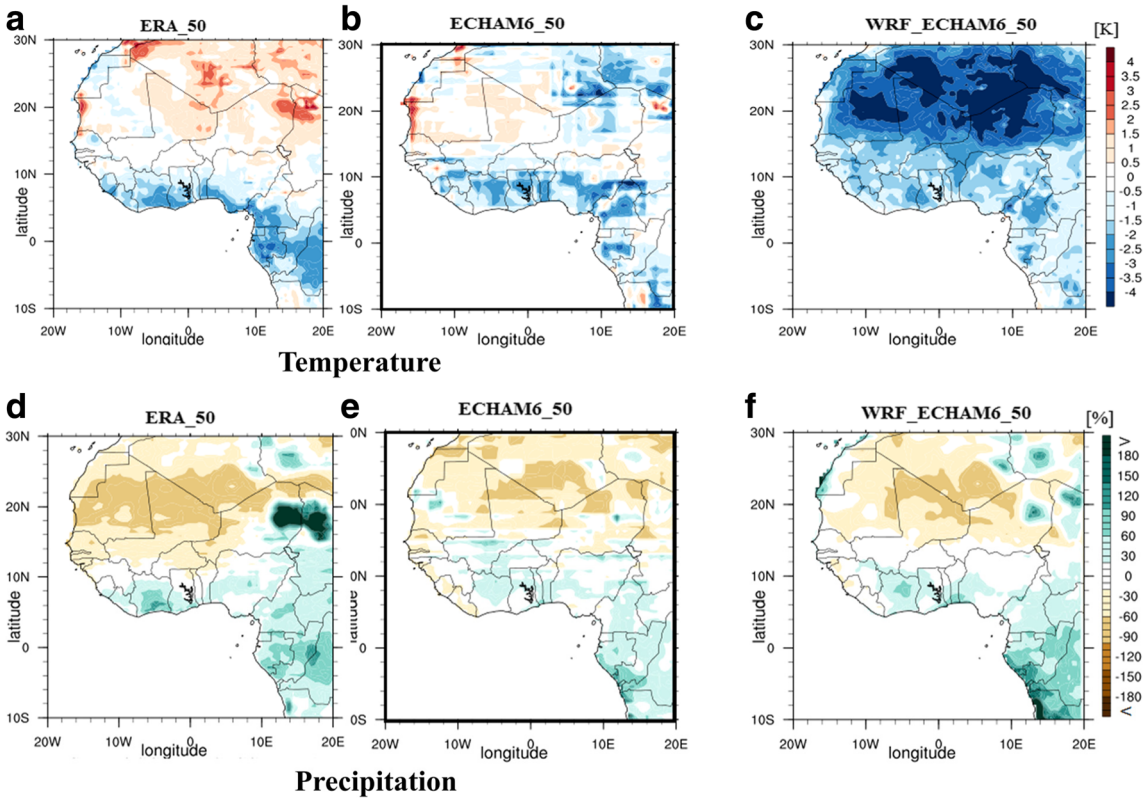

Fig. 9 Difference (i.e., model minus observation) maps of 1980–2005 climatology of annual mean temperature (**a**–**c**) and annual total precipitation (**d**–**f**) for ERA_50 (**a**, **d**), ECHAM6_50 (**b**, **e**), and WRF_ECHAM6_50 (**c**, **f**), in comparison to CRU data for temperature and GPCC data for precipitation. NCAR Command Language (NCL) package was used for this figure

Coast for both the GCM realization and the RCM run could be attributed to a significant representation by the models, of the supply of moist air from the nearby sea. In contrast, areas such as the Sahara region, predominantly desert area, the models in general show dry bias. For the Soudano-Sahel and the Sahel regions, significant parts of the areas have nearly null bias, demonstrating the WRF's ability to simulate observed precipitation better than the MPI-ESM over this area. In general, the RCM simulations have null bias for larger areas than the forcing data sets. This result is consistent with RCM simulations performed by Jung and Kunstmann (2007), Frei et al. (2003), Vigaud et al. (2011), Boberg et al. (2010), and Berg et al. (2013). The wet bias scattered in the eastern part of the Sahara region in the GCM is rather intensified by the RCM, probably due to an excess simulation of precipitation over mountainous area in WRF.

3.2.2 Inner domain temperature and precipitation results

The top panel of Fig. 10a, b shows the biases of the annual mean 2-m temperature with respect to the 1980–2005 climatology over the Volta Basin in the inner domain. Temperature, in general, is underestimated in the MPI-ESM simulation (in figure named ECHAM6_10) by a mean bias of around −1.3 K. The general underestimation of temperature over the Volta Basin is further increased to a mean bias of about −1.8 K in the WRF_ECHAM6_10 simulation. However, the WRF model reduces the cold bias around most parts of the Volta Lake from about −2.5 K in the GCM to around −1.0 K. This demonstrates the ability of the RCM to capture the influence of the world's largest man-made lake on temperature better due to increase in horizontal resolution. In some parts of the Sahel, the RCM increases the bias from nearly zero for the GCM to about −2.5 K. No additional bias is introduced as a result of the WRF nesting simulation, since biases in 2-m temperature in both nests over the basin are almost similar.

In Fig. 11, the spatial biases in the climatological mean on the seasonal scale for temperature are shown. The GCM strongly underestimates the observed temperature (bias around −4.5 K) over almost the entire basin especially the GC and SS belts for the DJF season. For the same season, the WRF_ECHAM6_10 simulation reduces the strong negative bias in the GCM (spatial mean bias of −4.4 K) over almost all areas of the basin (spatial mean bias of −3.0 K for the WRF). Also, the WRF_ECHAM6_10 simulation adds value to the GCM simulation of the JJA season temperature (spatial mean bias of 1.1 for the GCM and −0.5 for the RCM). The GCM in general overestimates the temperature in the SH and SS zones, but biases are close to zero over most parts of the GC. For the RCM, the temperature in the SH (GC) area is slightly overestimated (underestimated), but bias close to zero is recorded for most parts of the SS. In the case of the SON season, both the GCM and the RCM simulate generally similar biases over the basin with spatial means of −1.6 K in both cases. Meanwhile, the strong underestimation of temperature over Ghana part of the basin is reduced in the RCM simulation. In the MAM season, biases are closer to zero in the GCM (especially in the northern and western parts) than the WRF_ECHAM6_10 simulation. The WRF model simulates strong negative bias over the northern part of the basin.

Table 4 summarizes the 1980–2005 climatological seasonal means in 2-m temperature over the Volta Basin of the inner domain for the MPI-ESM driven WRF simulations (WRF_ECHAM6_10 and _50) and the ECHAM6 realization (ECHAM6_10). On annual time scales, both the GCM realization and the RCM simulation produce cold biases, although the cold bias is intensified in the WRF output. Among all seasons, summer is the only season where there are opposite signs of the mean biases for the ECHAM6_10 (1.1 K) and the WRF_ECHAM6_10 (−0.5 K) simulation. All other seasons have a negative sign for the mean bias in both cases. Moreover, while the RCM downscaling reduces the mean biases for winter and summer, it increases the spring bias and maintains a similar bias for autumn (−1.6 K). Although both the MPI-ESM and the WRF exhibit the largest biases in winter, the range in the seasonal mean biases is smaller in the RCM (−0.5 to −3.0 K) than in the GCM (−0.3 to −4.4 K).

The results for the interannual variability in 2-m temperature averaged over the basin are given in the top panel of Fig. 5. In general, the ECHAM6_10 and the WRF_ECHAM6_10 simulation have similar patterns in the interannual variability in the temperature over the basin, which reasonably reproduce the observed pattern, though biases in the amplitude of the interannual variability are quite large especially in the case of the GCM. The amplitudes of the inter-annual variability of both the GCM and the RCM are opposite in sign to that of the observed data for 1982–1985, 1987, and 1998–2001. However, both models simulate quite similar in value and pattern as the observed for the 1988–1996 period especially in the WRF_ECHAM6_10 simulation. The WRF_ECHAM6_10 simulation therefore added value to the simulation of the interannual variability of temperature by GCM over the basin.

The results for total annual precipitation (Fig. 10c, d) indicate relative biases between 0 and 60% over the Volta Basin in the GCM, and from −10 to 90% in the RCM experiment. The WRF model increases the wet bias in most areas of both the Guinea Coast and the western Soudano-Sahel regions, but decreases the wet bias to nearly zero over most areas of the northern part of the Sahel. The RCM nested downscaling simulation contributes to the systematic bias in precipitation, similar to our findings from the ERA-Interim downscaling experiment. A possible source of the systematic biases in both temperature and precipitation is the land surface model (LSM). It is known that RCMs employ LSMs with usually higher-resolution vegetation maps that are not present in GCMs (e.g., Vigaud et al. 2011) and, therefore, reproduce surface-atmosphere interactions differently.

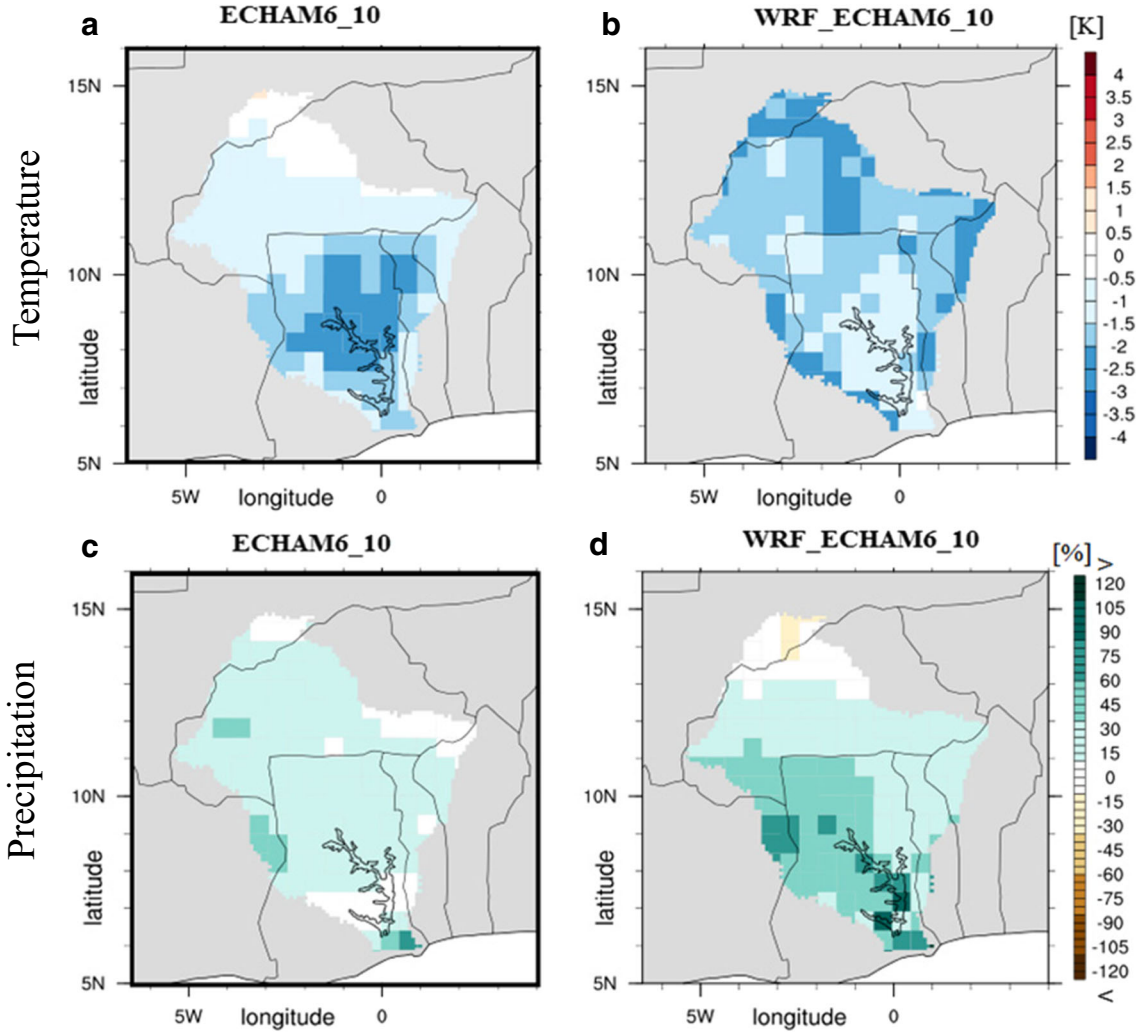

Fig. 10 Difference (i.e., model minus observation) maps of 1980–2005 climatology of annual mean temperature (**a**, **b**) and annual total precipitation (**c**, **d**) for the ECHAM6_10 (**a**, **c**) and WRF_ECHAM6_10 (**b**, **d**), in comparison with CRU data for temperature and GPCC data for precipitation for the Volta Basin. NCAR Command Language (NCL) package was used for this figure

In Fig. 12, the spatial biases for the period climatological mean of seasonal total precipitation are shown. In general, similar patterns in bias are simulated by the GCM and the RCM for all the seasons. For the DJF season, both the GCM and the RCM underestimate the observed precipitation over the entire basin. The negative bias is larger in the GCM than the WRF_ECHAM6_10 simulation. In the case of the MAM season, both the GCM and RCM simulate biases close to zero for most parts of the basin. However, the RCM strengthens the positive bias the GCM simulates in the north most part of the basin, but simulates a weak dry over a smaller area than the GCM. Both the GCM and the RCM record positive bias mostly in the southwestern parts of the basin and biases from zero to about −15% in the northeastern areas of the basin for the JJA season. In the SON season, the GCM simulates wet bias over the entire basin, with the strongest bias in the northwestern side of the area. Similar to the forcing data, positive bias is simulated by the RCM over almost the entire basin, but in the case of the RCM, the intensification of the positive bias is in the south and the western parts of the basin. In all the four seasons, the biases in the GCM (either dry or wet) are generally carried over to the RCM simulation, but the spatial patterns in the bias differ somehow, except the DJF season. This shows that the WRF model simulates precipitation quite different from the GCM over the Volta basin; however, the simulated precipitation by the RCM is influenced to some extent by the GCM confirming the effect of a one-way nesting dynamical downscaling process mentioned by Giorgi and Gutowski (2015).

In Fig. 13, the ECHAM6_10 (a) and the WRF_ECHAM6_10 (b) of the 1980–2005 climatological mean bias results for April total precipitation are shown. The spatial distribution of the relative bias does not differ largely in both the GCM and the RCM simulations. However, the RCM reduces the spatial mean bias from about 9% (for the GCM) to 0% for the Volta Basin in the inner domain simulation, indicating the added value of the

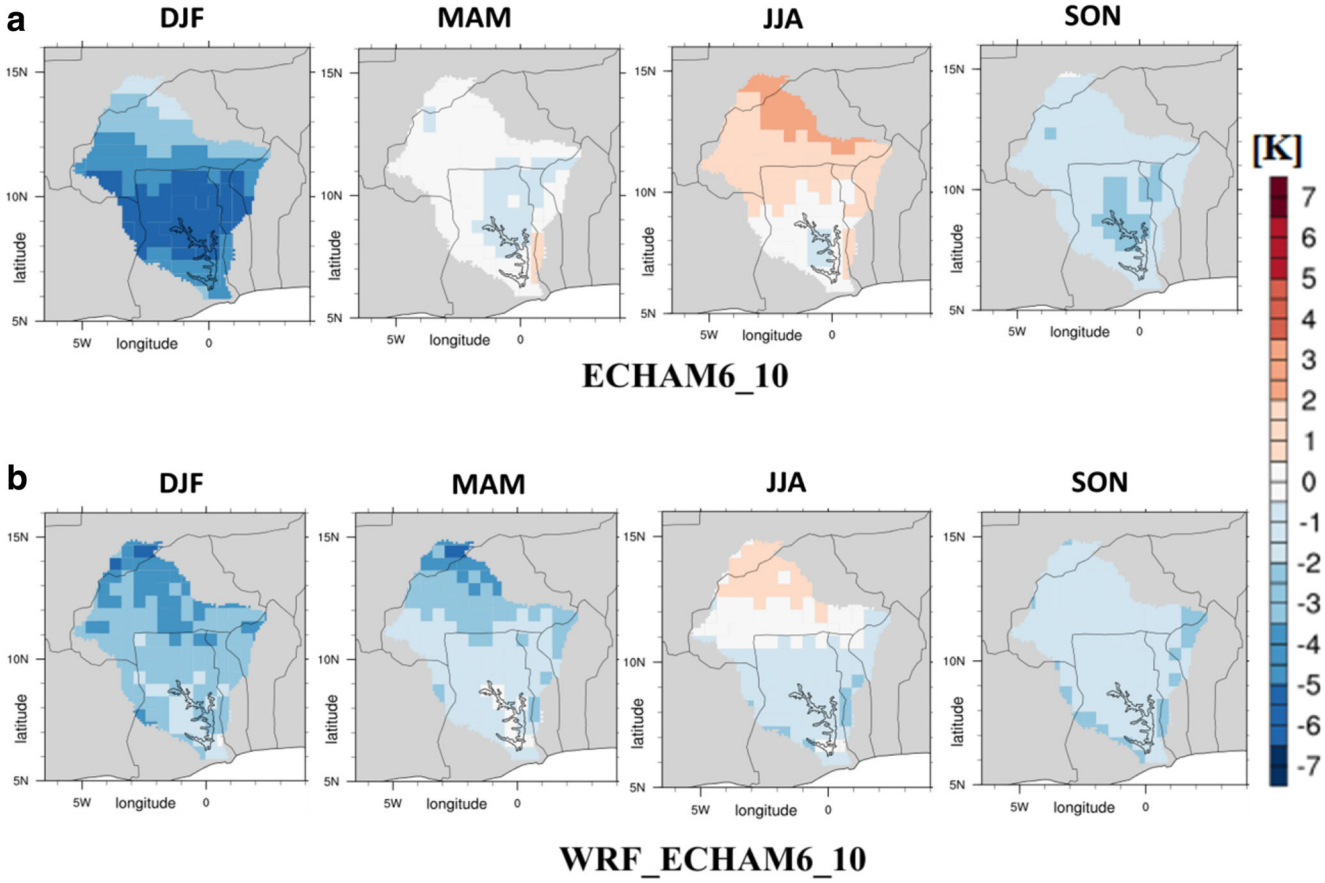

Fig. 11 Difference (i.e., model minus observation) maps of 1980–2005 climatology mean of seasonal mean temperature for ECHAM6_10 (**a**) and the WRF_ECHAM6_10 (**b**) simulation in comparison to CRU data over the Volta Basin. NCAR Command Language (NCL) package was used for this figure

WRF_ECHAM6_10 simulation of the April precipitation. A noticeable difference, however, in the GCM and RCM results is in the eastern part of the Soudano-Sahel region, where a slightly wet bias (for the GCM) and nearly zero/slightly dry bias (for the RCM) are visible. A comparison of the results for April between WRF_ERA_10 and the WRF_ECHAM6_10 indicates that the simulated biases of the RCM might be influenced by the driving large-scale data, since the WRF model is giving a divergent result when the model is forced by the two large-scale data.

The biases in total precipitation with respect to the 1980–2005 climatological mean on both seasonal and annual time scales and separately for April are provided in Table 5. For the three subregions as well as for to the whole Volta Basin, both the GCM and the RCM produce wet biases on annual time scale and for summer and autumn and dry biases for winter. As discussed previously, this can be attributed to the fact that the summer monsoon precipitation is simulated better than the winter season precipitation. The dry biases simulated for the winter season by both the GCM and the RCM (including the simulation where WRF is driven by the reanalysis data) are generally large, but slightly reduced in the RCM simulations. This result shows that significantly low amounts of precipitation are simulated in winter by the MPI-ESM and that this underestimation of precipitation is passed on to WRF through the relevant atmospheric moisture fields (Annor 2015). For April, the WRF_ECHAM6_10 simulation decreases the GCM bias from about 9% to around zero for the whole Volta Basin, from −4% to −3% for the Guinea Coast, and from 42 to 33% for the Sahel. It is only in the Soudano-Sahel region of the basin where the WRF_ECHAM6_10 simulation intensifies the bias from 5 to −12%. These biases are generally low for April in both the GCM and the RCM, which stands in contrast to the WRF_ERA_10 simulation. This illustrates again the influence of the driving data on the RCM downscaling process. For spring, the MPI-ESM

Table 4 Inner domain seasonal and annual mean 2-m temperature bias [K] in comparison to CRU temperature version TS3.21, averaged over the whole Volta Basin from 1980 to 2005 for WRF_ECHAM6_10, WRF_ECHAM6_50, and the MPI-ESM model output over the basin (ECHAM6_10)

Simulation	DJF	MAM	JJA	SON	Annual
WRF_ECHAM6_10	−3.0	−1.9	−0.5	−1.6	−1.8
WRF_ECHAM6_50	−3.0	−1.8	−0.3	−1.5	−1.7
ECHAM6_10	−4.4	−0.3	1.1	−1.6	−1.3

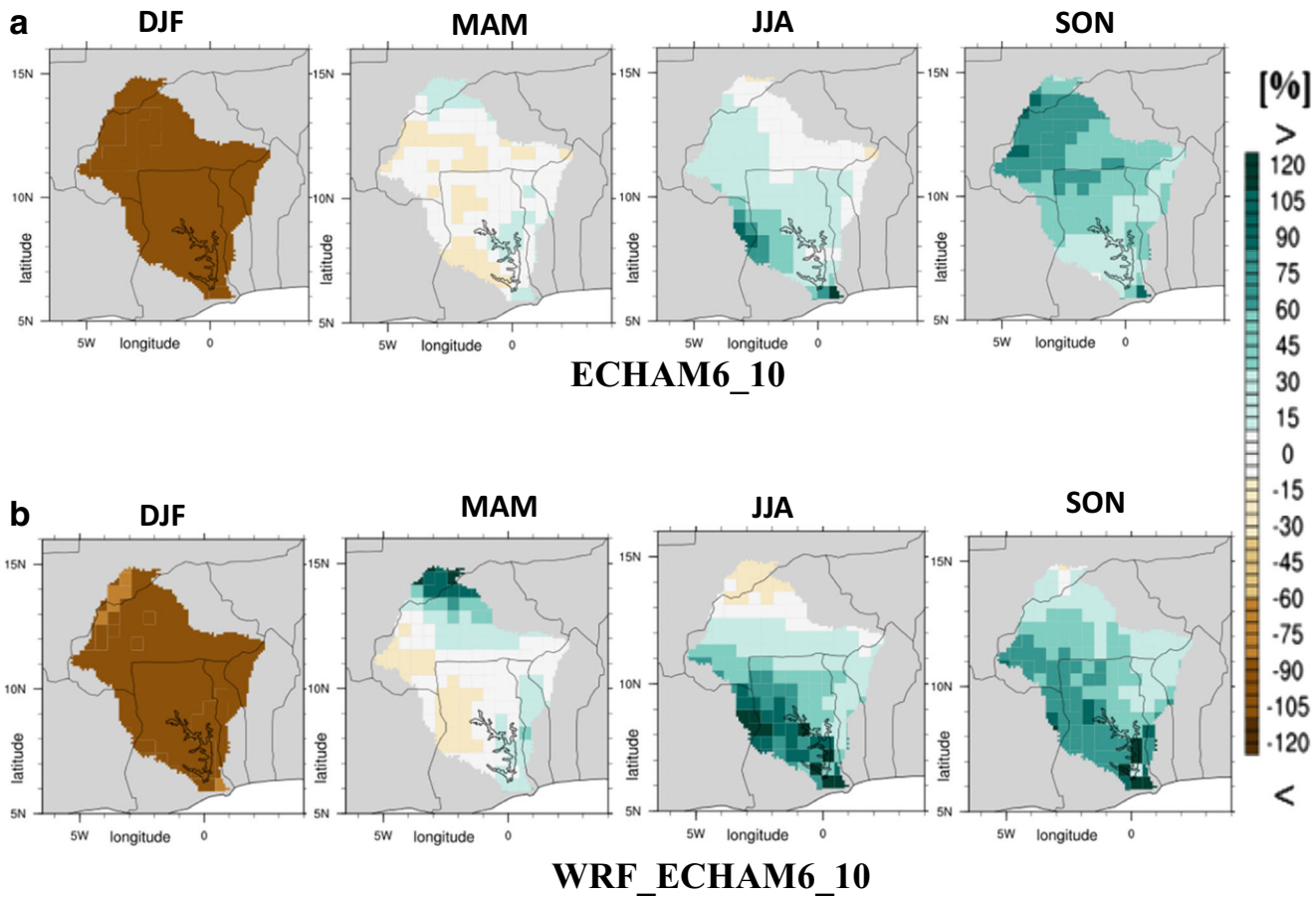

Fig. 12 Difference (i.e., model minus observation) maps of 1980–2005 climatology mean of seasonal total precipitation for ECHAM6_10 (**a**) and the WRF_ECHAM6_10 (**b**) simulation in comparison with GPCC data over the Volta Basin. NCAR Command Language (NCL) package was used for this figure

underestimates the precipitation for the whole Volta Basin (−2%), the Guinea Coast (−3%), and the Soudano-Sahel regions (−3%). The WRF model in the 10-km domain overestimates the precipitation for the whole Volta Basin (12%), the Guinea Coast (5%), and produces nearly zero bias for the Soudano-Sahel. Both the GCM and the RCM overestimate precipitation over the Sahel, while the wet bias is strengthened in the downscaling process.

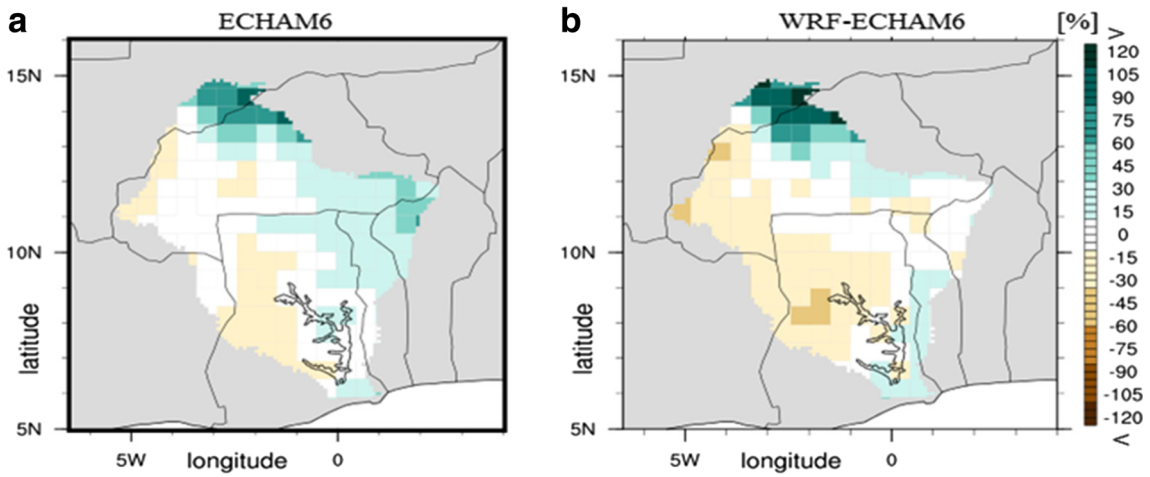

Fig. 13 Difference (i.e., model minus observation) maps of 1980–2005 climatology of April total precipitation for ECHAM6_10 (**a**) and the WRF_ECHAM6_10 (**b**) in comparison with GPCC data for the Volta Basin. NCAR Command Language (NCL) package was used for this figure

Table 5 April, seasonal, and annual total precipitation relative bias [%] of the inner domain, in comparison with GPCC version 6.0 data, averaged over the entire Volta Basin (VB), the Guinea Coast (GC), the Soudano-Sahel (SS), and the Sahel (SH) regions of the Volta Basin from 1980 to 2005 for WRF driven by MPI-ESM (WRF_ECHAM6_10 and WRF_ECHAM6_50) simulations and the MPI-ESM model output (ECHAM6_10)

Simulation	April	DJF	MAM	JJA	SON	Annual
WRF_ECHAM6_10 (VB)	0	−96	12	40	51	31
WRF_ECHAM6_50 (VB)	−19	−97	−7	21	29	12
ECHAM6_10 (VB)	9	−97	−2	21	50	20
WRF_ECHAM6_10 (GC)	−3	−94	5	90	85	54
WRF_ECHAM6_10 (GC)	−15	−94	−9	64	61	32
ECHAM6_10 (GC)	−4	−98	−3	38	29	15
WRF_ECHAM6_10 (SS)	−12	−97	0	46	53	35
WRF_ECHAM6_50 (SS)	−29	−98	−17	25	30	15
ECHAM6_10 (SS)	5	−98	−3	25	48	22
WRF_ECHAM6_10 (SH)	33	−94	44	3	29	7
WRF_ECHAM6_50 (SH)	5	−96	18	−15	8	−8
ECHAM6_10 (SH)	42	−95	1	8	67	19

The results for the interannual variability in precipitation averaged over the basin are given in the bottom panel of Fig. 5. The patterns in the interannual variability are similar for the GCM output and WRF_ECHAM6_10 simulation, but the biases in the WRF_ECHAM6_10 are smaller than the ECHAM6_10 output indicating an added value by the downscaling process. Both the GCM and the RCM are able to reproduce the pattern in the variability well in some cases (1980–1984, 1988–1990, 1992–1993, and 2000–2005), but the interannual variability for both the GCM and the RCM are out of phase of that of the observed for most of the remaining years. Although the GCM and the RCM reasonably capture the observed driest year (1983) and wettest year (2003), both the GCM and the RCM simulate 1982 as the driest year and 1999 as the wettest year.

3.2.3 Taylor diagrams

To assess the performance of the RCM in reproducing the spatial patterns of the observed total precipitation data from GPCC on seasonal scale, Taylor diagrams (Taylor 2001) were plotted for the whole Volta Basin (Fig. 14) and the three belts of the basin (Fig. 15) for the inner domain simulations.

For the whole Volta Basin (Fig. 14), the performance of the model varies for the four seasons. For the winter and spring seasons, spatial correlations are low (0.41 and 0.44, respectively). On the contrary, the WRF model has high spatial correlations for the summer (0.66) and the autumn (0.88) seasons. On the other hand, least and underestimation of spatiotemporal variability ($\sigma < 0.5$) is produced for winter, whereas the spatiotemporal variability is overestimated ($\sigma > 1.5$) for the other three seasons. The spatial distribution of precipitation in our simulations is in line with previous simulations with the WRF model over West Africa (e.g., Noble et al. 2014).

From Fig. 14, we infer that both the MPI-ESM and the WRF model have quite similar spatial pattern correlations with the observation data (positive correlations increasing from as low as 0.02 to 0.81 in the order winter, spring, summer, and autumn) for all the four seasons over the whole basin. Interestingly, except for the winter season where both the GCM and the RCM are underestimating the observed standard deviation equally and have similar RMS errors, the WRF downscaling experiment further overestimates the observed standard deviation and has larger RMS errors for the rest of the seasons. The spatial correlations are in similar ranges to that of the WRF_ERA_10 simulations, although the latter has the highest correlation for all seasons. With the exception of winter, all simulations are overestimating the observed standard deviation.

In winter (Fig. 15), the spatial correlations with observations are low, ranging from about 0.24 to 0.56, with underestimation of the observed standard deviation. Conversely, the observed spatiotemporal variability is overestimated ($\sigma > 1.25$) for the other three seasons over all zones. In spring, pattern correlations of about 0.50, 0.36, and 0.60 are achieved for GC, SS, and SH. Spatial pattern correlations in summer (autumn) of about 0.49 (0.71) for GC, 0.70 (0.84) for SS, and 0.62 (0.82) for SH are obtained for the RCM. The spatial pattern correlation decreases from South to North (i.e., GC to SH) during winter, while it does not follow any specific patterns for the other three seasons. Over the three sub-regions, highest correlations are produced in autumn and lowest for winter. However, the smallest spread in spatio-temporal variability (and also in correlation) is simulated for winter, while the largest spread in these statistical parameters is produced for spring. In winter, the entire region of West Africa experiences the dry effect of the trade winds, and therefore, convective activities are spatially uniform over the region and minimal even at subgrid levels. Thus, the RCM driven by the ERA-Interim simulated the convective precipitation processes almost the same across the whole region, which could be the reason for the least spread in correlation and standard deviation in winter over all regions in the basin. On the other hand, convective activities spatially, temporally, and even in intensity prevail randomly in spring over the entire region; hence, there exits maximum spatial variability in the way in which the RCM simulates these processes.

For the three subregions (Fig. 15) and for both the GCM and the RCM (also that of the WRF_ERA_10), spatial correlations with observations are generally low for winter, high for autumn, and in between for spring

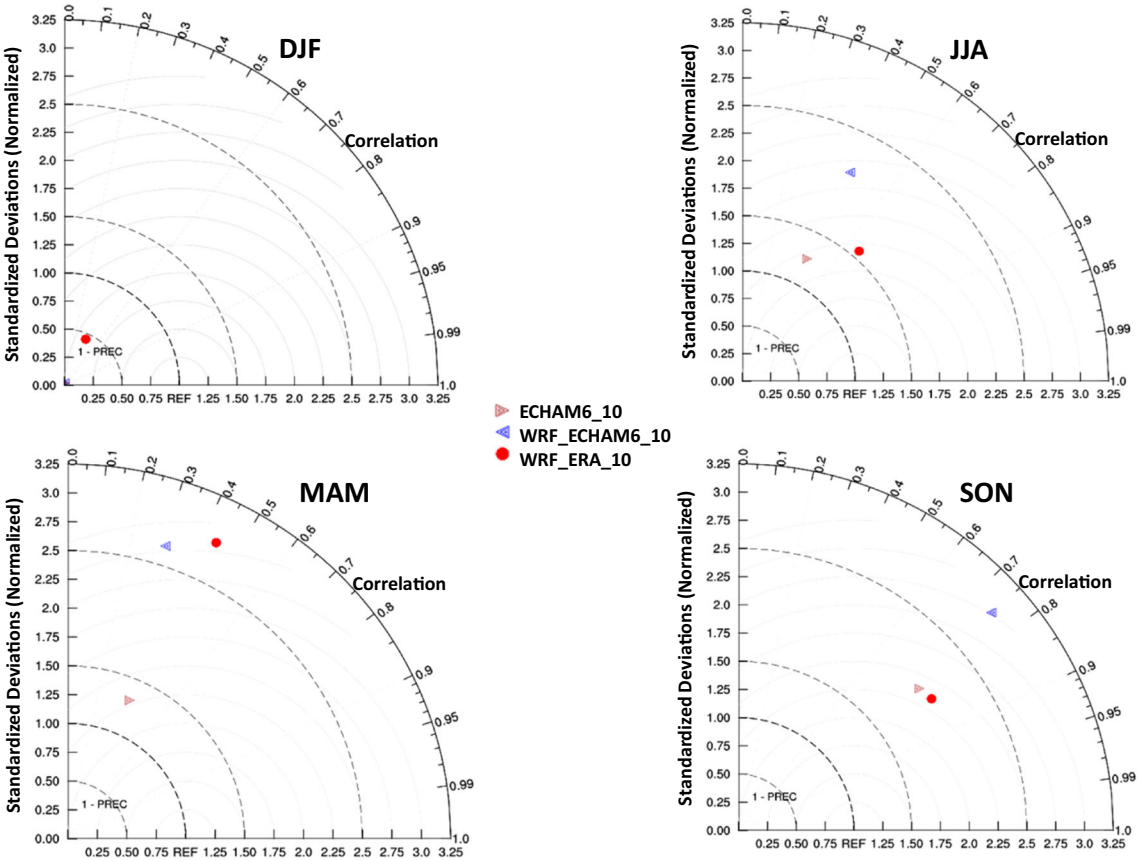

Fig. 14 Taylor diagrams of seasonal total precipitation for the Volta Basin, using GPCC data set as reference. The results for the WRF_ERA_10, WRF_ECHAM6_10, and the ECHAM6_10 for the entire Volta Basin are indicated with a *red circle*, *blue* and *brown triangles*, respectively, for each season. NCAR Command Language (NCL) package was used for this figure

and summer. It is worth noting that except for autumn, the spatial correlation over the Guinea Coast for both the GCM and the RCM are lower than the other two regions. Both MPI-ESM and WRF (as well as the WRF_ERA_10 simulation) are underestimating (overestimating) the winter (autumn) observed standard deviation for all the regions. The largest spread in standard deviation (and also in correlation) for all subregions and in all simulations is found in spring, followed by summer, autumn, and winter as the season with the least spread in these parameters. These findings can be linked to the fact that in winter, the whole West African region is under the influence of a dry trade wind and, consequently, subgrid convective activities are minimal and spatially uniform. Hence, the simulation of subgrid convective activities by the RCM do not differ much from the GCM simulation across the entire region. This is in contrast to the spring season, where convective activities prevail stochastically on spatial and temporal scale and in intensity, and therefore, larger differences are found in the way the GCM and the RCM simulate the subgrid convective activities over different parts of the region (see also Annor 2015).

4 Summary and conclusions

Long-term (1980–2005) high-resolution RCM simulations were performed over the Volta Basin in the West African region using the WRF model. We applied a one-way nested approach with the outer and inner domains at 50 and 10 km, respectively, where the WRF was used to downscale both the MPI-ESM (ECHAM 6) model output and the ERA-Interim re-analysis data over West Africa and the Volta Basin.

In general, GCM biases were transferred to the RCM, but we also identified additional contributions to the biases from the RCM itself. Furthermore, for the nesting configuration used here, the biases in temperature in the parent domain are propagated unchanged into the nested domain. For precipitation, on the other hand, the nested simulations further increased the mean biases in most cases a problem that could be attributed to the effect of one-way nesting and internal model physics. While the WRF model strengthens the cold bias especially for most of the Sahel and the Sahara regions, the mean dry bias in precipitation produced by the MPI-ESM is reduced in the WRF_ECHAM6_50 simulation. Over the Volta Basin

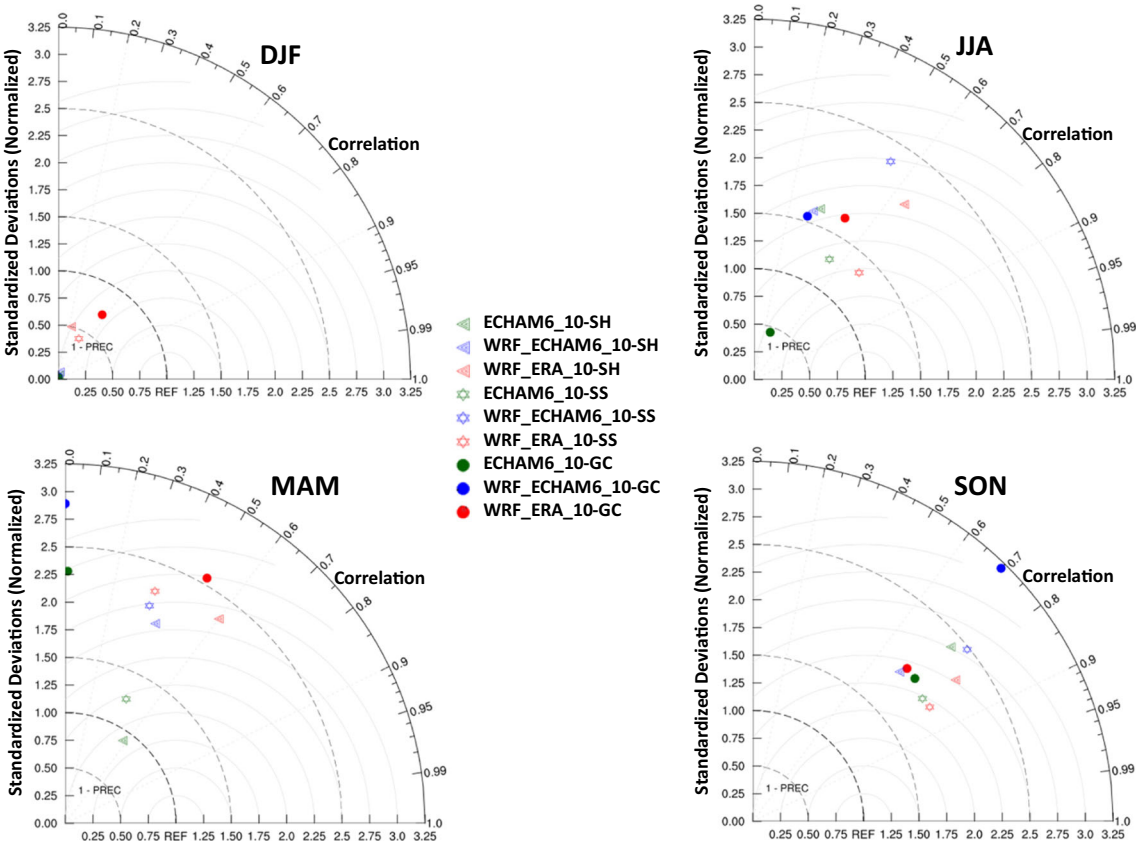

Fig. 15 Taylor diagrams of seasonal total precipitation for the Guinea Coast (GC), Soudano-Sahel (SS), and Sahel (SH) regions of the Volta Basin, using GPCC data set as reference. The *red circles*, *stars*, and *triangles* are the seasonal results of the WRF_ERA_10, spatially averaged over the Guinea Coast (GC), Soudano-Sahel (SS), and the Sahel (SH) regions of the Volta Basin. The *blue* (*green*) *circles*, *stars*, and *triangles* are WRF_ECHAM6_10 (ECHAM6_10) seasonal results for the Guinea Coast, the Soudano-Sahel, and the Sahel, respectively, of the basin. NCAR Command Language (NCL) package was used for this figure

region, WRF produced the strongest bias for winter temperature and weakest for summer temperature, and in both seasons, the RCM mean biases in temperature are all smaller than that of the GCM. Also for precipitation, summer bias is far smaller than winter, and interestingly for the month of April, the performance of the WRF model is well demonstrated by simulating nearly a null bias for the basin, and again, almost a zero bias for spring over the Soudano-Sahel region of the basin.

In the case of the inter-annual variability over the whole basin, both the WRF and MPI-ESM simulate in most cases similar patterns; however, biases are smaller in the WRF simulation than that of the MPI-ESM for both temperature and precipitation.

Spatial correlations of simulated precipitation with the observed climatological mean for the entire Volta Basin and the three agroclimatical subregions Guinea Coast, Soudano-Sahel, and Sahel are high (0.7–0.8) for autumn and low (0.0–0.2) for winter. In all simulations, the largest spread in the standard deviation (and also in correlation) for all the subregions as well as the entire Volta Basin is found in spring, followed by summer, autumn, and winter as the season with the least spread in these parameters.

Vigaud et al. (2011) reported an excess of about 25% in 1981–1990 mean JAS precipitation for a similar region as the coarse domain in this study, when the WRF was driven by ERA-40 re-analysis data. In comparison, our results for both summer (JJA) and autumn (SON) precipitation for the coarse domain indicate that relative biases are smaller (around −13% for summer and 7% for autumn). For a similar domain configuration of a coarser domain over West Africa and a finer domain over the Volta Basin, Jung and Kunstmann (2007) dynamically downscaled the NCEP re-analysis data for 1997 using the MM5 RCM and reported temperature biases between −2 and 2 °C (see their Fig. 6) for the Volta Basin. Hence, from our assessment of the biases in both near surface temperature and precipitation on annual and seasonal scales with respect to the 1980–2005 climatological means, we conclude that our current high-resolution simulations are up to par with other state-of-the-art simulations over West Africa (e.g., Nikulin et al. 2012; Giorgi and Gutowski 2015). In addition, the WRF downscaling simulation is suitable for the investigations of future climate projection.

Acknowledgements This study was financially supported by the German Federal Ministry of Education and Research (BMBF) within the framework of the West African Science Service Centre on Climate Change and Adapted Land Use (WASCAL) project. We gratefully acknowledge the funding of the work. The authors are thankful to staff members of the German Climate Centre (DKRZ) and the Institute of Meteorology and Climate Research Atmospheric Environmental Research (IMK-IFU) for, respectively, providing high performance computing facilities and other important tools that were used to perform this regional climate simulation with the WRF model. We appreciate the contributions of the WRF community for the provision of the WRF codes, Maxwell Planck's Institute (MPI), and the European Centre for Medium-range Weather Forecasting (ECMWF) for providing the forcing data. We acknowledge the usefulness of the observed gridded temperature data from the Climate Research Unit (CRU) and precipitation from the Global Precipitation Climatology Centre (GPCC), Deutscher Wetterdienst (DWD).

References

Afiesimama EA, Pal JS, Abiodun BJ, Gutowski WJ Jr, Adedoyin A (2006) Simulation of west African monsoon using the RegCM3. Part I: model validation and interannual variability. Theor Appl Climatol 86:23–37

Amisigo BA (2005) Modelling riverflow in the Volta Basin of West Africa: a data-driven framework. Ecology and development series no. 34, Cuvillier Verlag Göttingen, 175 pp.

Annor T (2015) Potential impacts of climate variability and change on hydrology and water resources over the Volta Basin. PhD Dissertation, Federal University of Technology Akure, Nigeria, 115 pp.

Bekoe EO (2013) The impact of droughts and climate change on electricity generation in Ghana. Environ Sci 1:13–24

Beljaars ACM (1994) The parameterization of surface fluxes in large-scale models under free convection. Quart J Roy Meteor Soc 121: 255–270

Berg P, Wagner S, Kunstmann H, Schädler G (2013) High resolution regional climate model simulations for Germany: part I-validation. Clim Dyn 40:40–414. doi:10.1007/s00382-012-1508-8

Boberg F, Berg P, Thejll P, Gutowski WJ, Christensen JH (2009) Improved confidence in climate change projections of precipitation evaluated using daily statistics from the PRUDENCE ensemble. Clim Dyn 32:1097–1106. doi:10.1007/s00382-008-0446-y1

Boberg F, Berg P, Thejll P, Gutowski WJ, Christensen JH (2010) Improved confidence in climate change projections of precipitation further evaluated using daily statistics from ENSEMBLES models. Clim Dyn 35:1509–1520. doi:10.1007/s00382-009-0683-8

Castro CL, Pielke RA, Leoncini G (2005) Dynamical downscaling: an assessment of value added using a regional climate model. J Geophys Res 110:D05108

Chen F, Dudhia J (2001) Coupling an advanced land-surface/hydrology model with the Penn State/NCAR MM5 modelling system. Part I: model implementation and sensitivity. Mon.Weather Rev 129:569–585

Dee DP, Uppala SM, Simmons AJ, Berrisford P, Poli P, Kobayashi S, Andrae U, Balmaseda MA, Balsamo G, Bauer P, Bechtold P, Beljaars ACM, van de Berg L, Bidlot J, Bormann N, Delsol C, Dragani R, Fuentes M, Geer AJ, Haimberger L, Healy SB, Hersbach H, Hólm EV, Isaksen L, Kållberg P, Köhler M, Matricardi M, McNally AP, Monge-Sanz BM, Morcrette J-J, Park B-K, Peubey C, de Rosnay P, Tavolato C, Thépaut J-N, Vitart F (2011) The ERA-interim reanalysis: configuration and performance of the data assimilation system. Quart J Roy Meteor Soc 137:553–597. ISSN 1477-870X. doi:10.1002/qj.828 (Part A)

Di Luca A, de Elia R, Laprise R (2012) Potential for added value in precipitation simulated by high resolution nested regional climate models and observations. Clim Dyn 38:1229–1247

Di Luca A, de Elia R, Laprise R (2013) Potential for small scale added value of RCM's downscaled climate change signal. Clim Dyn 40: 1415–1433

Dinku T, Connor SJ, Ceccato P, Ropelewski CF (2008) Comparison of global gridded precipitation products over a mountainous region of Africa. Int J Climatol 28:1627–1638

Dudhia J (1989) Numerical study of convection observed during the winter monsoon experiment using a mesoscale two–dimensional model. J Atmos Sci 46:3077–3107

Dyer AJ, Hicks BB (1970) Flux–gradient relationships in the constant flux layer. Quart J Roy Meteor Soc 96:715–721

Fekete BM, Vörösmarty CJ, Roads JO, Willmott CJ (2004) Uncertainties in precipitation and their impacts on runoff estimates. J Clim 17: 294–304

Feser F (2006) Enhanced detectability of added value in limited-areamodel results separated into different spatial scales. Mon Weather Rev 134:2180–2197

Frei C, Christensen JH, Déqué M, Jacob D, Jones RG, Vidale PL (2003) Daily precipitation statistics in regional climate models: evaluation and intercomparison for the European alps. J Geophys Res 108: 4124–4143. doi:10.1029/2002JD002287

Giorgetta M, Jungclaus J, Reick C, Legutke S, Brovkin V, Crueger T, Esch M, Fieg K, Glushak K, Gayler V, Haak H, Hollweg H, Kinne S, Kornblueh L, Matei D, Mauritsen T, Mikolajewicz U, Müller W, Notz D, Raddatz T, Rast S, Roeckner E, Salzmann M, Schmidt H, Schnur R, Segschneider J, Six K, Stockhause M, Wegner J, Widmann H, Wieners K-H, Claussen M, Marotzke J, Stevens B (2012) CMIP5 simulations of the max Planck Institute for Meteorology (MPI-M) based on the MPI-ESM-MR model: the historical experiment, served by ESGF. World Data Center Clim (WDCC). doi:10.1594/WDCC/CMIP5.MXMRhi

Giorgetta MA, Roeckner E, Mauritsen T, Bader J, Crueger T, Esch M, Rast S, Kornblueh L, Schmidt H, Kinne S, Hohenegger C, Möbis B, Krismer T, Wieners KH, Stevens B (2013) The atmospheric general circulation model ECHAM6 model description. Reports on Earth System Science, MPI-M, Germany. ISSN 1614-1199

Giorgi F (2006) Regional climate modeling: status and perspectives. J Phys IV France 139:101–118. doi:10.1051/jp4:2006139008

Giorgi F, Gutowski WJ Jr (2015) Regional dynamical downscaling and the CORDEX initiative. Annu Rev Environ Resour 40:467–490

Giorgi, F, Coppola, E, Solmon, F, Mariotti, L, Sylla, MB, Bi, X, Elguindi, N, Diro, GT, Nair, V, Giuliani, G, Turuncoglu, UU, Cozzini, S, Güttler, I, O'Brien, TA, Tawfik, AB, Shalaby, A, Zakey, AS, Steiner, AL, Stordal, F, Sloan, LC, Brankovic, C (2012) RegCM4: model description and preliminary tests over multiple CORDEX domains. Clim. Res. 52: 7–29. doi:10.3354/cr01018

Grell GA, Devenyi D (2002) A generalized approach to parameterizing convection combining ensemble and data assimilation techniques Geophys Res Lett 29(14)

Grell GA, Dudhia J and Stauffer DR (1995) A description of the fifth-generation Penn State/NCAR Mesoscale model (MM5), NCAR tech. Note NCAR/TN-398+STR, Natl. Cent. For Atmos. Res., boulder, Colo

Gruber A, Su X, Kanamitsu M, Schemm J (2000) The comparison of two merged rain gauge–satellite precipitation datasets. Bull Amer Meteor Soc 81:2631–2644

Harris I, Jones PD, Osborn TJ, Lister DH (2013) Updated high-resolution grids of monthly climatic observations - the CRU TS3.10 dataset. Int J Climatol. doi:10.1002/joc.3711

Hong SY, Dudhia J, Chen SH (2004) A revised approach to ice microphysical processes for the bulk parameterization of clouds and precipitation. Mon Weather Rev 132:103–120

IPCC (2001) Climate change 2001: the scientific basis is the most comprehensive and up-to-date scientific assessment of past, present and future climate change. The report. In: Houghton JT, Ding Y, Griggs DJ, Noguer M, van der Linden PJ, Dai X, Maskell K, Johnson CA (eds) contribution of working group I to the third assessment report of the intergovernmental panel on climate change. Cambridge University press, Cambridge

IPCC (2007) Climate change 2007: the physical science basis. In: Solomon S, Qin D, Manning M, Chen Z, Marquis M, Averyt KB, Tignor M, Miller HL (eds) Contribution of working group I to the fourth assessment report of the intergovernmental panel on climate change. Cambridge University Press, Cambridge

IPCC (2013) Climate change 2013 the physical science basis: in: stocker TF, Qin D, Plattner G-K, Tignor MMB, Allen SK, Boschung J, Nauels a, Xia Y, Bex V, Midgley PM contribution of working group I to the fifth assessment report of the intergovernmental panel on climate change summary for policymaker. IPCC, Switzerland. www.Ipcc.Ch and the IPCC WGI AR5 website www.climatechange2013.org

Jung G, Kunstmann H (2007) High-resolution regional climate modeling for the Volta region of West Africa. J Geophy Res 112:D23108. doi:10.1029/2006JD007951

Jung G, Wagner S, Kunstmann H (2012) Joint climate–hydrology modeling: an impact study for the data-sparse environment of the Volta Basin in West Africa. Hydrol Res 43(3):231–248

Kasei, AR (2009) Modeling impacts of climate change on water resources in the Volta Basin, West Africa. Ph.D. thesis, 195 pp., University of Bonn, Germany

Katragkou E, García-Díez M, Vautard R, Sobolowski S, Zanis P, Alexandri G, Cardoso RM, Colette A, Fernandez J, Gobiet A, Goergen K, Karacostas T, Knist S, Mayer S, Soares PMM, Pytharoulis I, Tegoulias I, Tsikerdekis A, Jacob D (2015) Regional climate hindcast simulations within EURO-CORDEX: evaluation of a WRF multi-physics ensemble. Geosci Model Dev 8:603–618

Kunstmann H, Jung G (2005) Impact of regional climate change on water availability in the Volta basin of West Africa. Regional Hydrological Impacts of Climatic Variability and Change (Proceedings of symposium S6 held 1 during the Seventh IAHS Scientific Assembly at Foz do Iguaçu, Brazil, April 2005). IAHS Publ 295, 2005

Mariotti L, Coppola E, Sylla MB, Giorgi F, Piani C (2011) Regional climate model simulations of projected 21st century climate change over an all-Africa domain: comparison analysis of nested and driving model results. J Geophys Res Atmos 116(D15):16

Mlawer EJ, Taubman SJ, Brown PD, Iacono MJ, Clough SA (1997) Radiative transfer for inhomogeneous atmospheres: RRTM, a validated correlated–k model for the longwave. J Geophy Res 102:16663–16682

Mooney PA, Mulligan FJ, Fealy R (2013) Evaluation of the sensitivity of the weather research and forecasting model to parameterization schemes for regional climates of europe over the period 1990–95. J. Clim 26:1002–1017

Neumann R, Jung G, Laux P, Kunstmann H (2007) Climate trends of temperature, precipitation and river discharge in the Volta Basin of West Africa. Intl. J. River Basin Manag 5:17–30

Nicholson SE, Some B, McCollum J, Nelkin E, Klotter D, Berte Y, Diallo BM, Gaye I, Kpabeba G, Ndiaye O, Noukpozounkou JN, Tanu MM, Thiam A, Toure AA, Traore AK (2003) Validation of TRMM and other rainfall estimates with a high-density gauge dataset for West Africa. Part I: Validation of GPCC Rainfall Product and Pre-TRMM Satellite and Blended Products. J Appl Meteorol 42:1337–1354

Nikulin G, Jones C, Giorgi F, Asrar G, Büchner M, Cerezo-Mota R, Christensen OB, Déqué M, Fernandez J, Hänsler A, van Meijgaard E, Samuelsson P, Sylla MB, Sushama L (2012) Precipitation climatology in an ensemble of CORDEX-Africa regional climate simulations. J Clim 25(18):6057–6078

Noble E, Druyan L, Fulakeza M (2014) The sensitivity of WRF daily summertime simulations over West Africa to alternative parameterizations. Part 1: African wave circulation. Mon Wea Rev 142:1588–1608. doi:10.1175/MWR-D-13-00194.1

Oguntunde PG, Abiodun BJ (2013) The impact of climate change on the Niger River basin hydroclimatology, West Africa. Clim Dyn 40:81–94. doi:10.1007/s00382-012-1498-6

Paeth H, Fink AH, Pohle S, Keis F, Mächel H, Samimi C (2011) Meteorological characteristics and potential causes of the 2007 flood in sub-Saharan Africa. Int J Climatol 31:1908–1926

Paulson CA (1970) The mathematical representation of wind speed and temperature profiles in the unstable atmospheric surface layer. J Appl Meteorol 9:857–861

Pleim JE (2007) A combined local and nonlocal closure model for the atmospheric boundary layer. Part I: Model Description and Testing. J Appl Meteor Climatol 46:1383–1395

Prein AF, Gobiet A, Truhetz H, Keuler K, Goergen K, Teichmann C, Fox Maule C, van Meijgaard E, Déqué M, Nikulin G, Vautard R, Colette A, Kjellström E, Jacob D (2016) Precipitation in the EURO-CORDEX 0.11° and 0.44° simulations: high resolution, high benefits? Clim. Dyn 46(1–2):383–412

Prömmel K, Geyer B, Jones JM, Widmann M (2010) Evaluation of the skill and added value of a reanalysis-driven regional simulation for alpine temperature. Int J Climatol 30:760–773

Raddatz TJ, Reick CH, Knorr W, Kattge J, Roeckner E, Schnur R, Schnitzler K-G, Wetzel P, Jungclaus J (2007) Will the tropical land biosphere dominate the climate-carbon cycle feedback during the twenty-first century? Clim Dyn 29:565–574

Roeckner E, Baeuml G, Bonaventura L, Brokopf R, Esch M, Giorgetta M, Hagemann S, Kirchner I, Kornblueh L, Manzini E, Rhodin A, Schlese U, Schulzweida U, Tompkins A (2003) The atmospheric general circulation model ECHAM 5. PART I: model description. Technical report, MPImet/MAD Germany

Roeckner E, Lautenschlager M, Schneider H (2006) IPCCAR4 MPI-ECHAM5 T63L31 MPI-OM GR1.5L40 SRESA2 run no.1: atmosphere 6 HOUR values MPImet/MaD Germany, world data Center for Climate, Hamburg, Alemanya. doi: 10.1594/WDCC/EH5-T63L31_OM-GR1.5L40_A2_1_6H

Roeckner E, Brokopf R, Esch M, Giorgetta M, Hagemann S, Kornblueh L, Manzini E, Schlese U, Schulzweida U (2006) Sensitivity of simulated climate to horizontal and vertical resolution in the ECHAM5 atmosphere model. J Clim 19:3771–3791. doi:10.1175/JCLI3824.1

Schneider U, Becker A, Finger P, Meyer-Christoffer A, Rudolf B, Ziese M (2011) GPCC full data reanalysis version 6.0 at 0.5°: monthly land-surface precipitation from rain-gauges built on GTS-based and historic data. doi:10.5676/DWD_GPCC/FD_M_V6_050

Senatore A, Mendicino G, Smiatek G, Kunstmann H (2010) Regional climate change projections and hydrological impact analysis for a Mediterranean basin in southern Italy. J Hydrol 399:70–92

Sijikumar S, Roucou P, Fontaine B (2006) Monsoon onset over Sudan-Sahel: simulations by regional scale model MM5. Geophys Res Lett 33. doi:10.1029/2005GL024819

Skamarock WC, Klemp JB, Dudhia J, Gill DO, Barker DM, Duda MG, Huang X, Wang W, Powers JG (2008) A description of the advanced research WRF version 3. Technical Report, NCAR, Boulder, Colorado, USA

Sylla MB, Gaye AT, Pal JS, Jenkins GS, Bi XQ (2009) High-resolution simulations of west African climate using regional climate model (RegCM3) with different lateral boundary conditions. Theor Appl Climatol 98:293–314. doi:10.1007/s00704-009-0110-4

Taylor KE (2001) Summarizing multiple aspects of model performance in a single diagram. J Geophy Res 106:7183–7192

Tewari M, Chen F, Wang W, Dudhia J, LeMone MA, Mitchell K, Ek M, Gayno G, Wegiel J, Cuenca RH (2004) Implementation and verification of the unified NOAH land surface model in the WRF model. 20th conference on weather analysis and forecasting/16th conference on numerical weather prediction 11–15

Torma C, Giorgi F, Coppola E (2015) Added value of regional climatemodeling over areas characterized by complex terrain—precipitation over the alps. J Geophys Res Atmos 120:3957–3972

Veljovic K, Rajkovic B, Fennessy MJ, Altshuler EL, Mesinger F (2010) Regional climate modeling: should one attempt improving on the large scales? Lateral boundary condition scheme: any impact? Meteorol Z 19:237–246

Vigaud N, Roucou P, Fontaine B, Sijikumar S, Tyteca S (2011) WRF/ARPEGE-CLIMAT simulated climate trends over West Africa. Clim Dyn 36:925–944

Webb EK (1970) Profile relationships: the log-linear range, and extension to strong stability. Quart J Roy Meteor Soc 96:67–90

Winterfeldt J, Weisse R (2009) Assessment of value added for surface marine wind speed obtained from two regional climate models. Mon Weather Rev 137:2955–2965

Zhang DL, Anthes RA (1982) A high-resolution model of the planetary boundary layer—sensitivity tests and comparisons with SESAME–79 data. J Appl Meteorol 21:1594–1609